Monthly Notices of the ROYAL ASTRONOMICAL SOCIETY
MNRAS **447,** 2348–2366 (2015) doi:10.1093/mnras/stu2561

Kepler photometry of RRc stars: peculiar double-mode pulsations and period doubling

P. Moskalik,[1⋆] R. Smolec,[1] K. Kolenberg,[2,3] L. Molnár,[4,5] D. W. Kurtz,[6] R. Szabó,[4] J. M. Benkő,[4] J. M. Nemec,[7] M. Chadid,[8] E. Guggenberger,[9,10] C.-C. Ngeow,[11] Y.-B. Jeon,[12] G. Kopacki[13] and S. M. Kanbur[14]

[1]*Copernicus Astronomical Center, ul. Bartycka 18, PL-00-716 Warsaw, Poland*
[2]*Harvard–Smithsonian Center for Astrophysics, 60 Garden Street, Cambridge MA 02138, USA*
[3]*Instituut voor Sterrenkunde, KU Leuven, Celestijnenlaan 200D, B-3001 Heverlee, Belgium*
[4]*Konkoly Observatory, MTA CSFK, Konkoly Thege Miklós út 15-17, H-1121 Budapest, Hungary*
[5]*Institute of Mathematics and Physics, Savaria Campus, University of West Hungary, Károlyi Gáspár tér 4, H-9700 Szombathely, Hungary*
[6]*Jeremiah Horrocks Institute, University of Central Lancashire, Preston PR1 2HE, UK*
[7]*Department of Physics & Astronomy, Camosun College, Victoria, BC V8P5J2, Canada*
[8]*Université Nice Sophia-Antipolis, Observatoire de la Côte d'Azur, UMR 7293, Parc Valrose, F-06108 Nice Cedex 02, France*
[9]*Max Planck Institut für Sonnensystemforschung, Justus-von-Liebig-Weg 3, D-37077 Göttingen, Germany*
[10]*Stellar Astrophysics Centre, Department of Physics and Astronomy, Aarhus University, Ny Munkegade 120, DK-8000 Aarhus C, Denmark*
[11]*Graduate Institute of Astronomy, National Central University, Jhongli 32001, Taiwan*
[12]*Korea Astronomy and Space Science Institute, 776, Daedeokdae-ro, Yuseong-gu, Daejeon 305-348, Korea*
[13]*Instytut Astronomiczny Uniwersytetu Wroclawskiego, Kopernika 11, PL-51-622 Wroclaw, Poland*
[14]*Department of Physics, SUNY Oswego, Oswego, NY 13126, USA*

Accepted 2014 December 1. Received 2014 November 28; in original form 2014 October 11

ABSTRACT

We present the analysis of four first overtone RR Lyrae stars observed with the *Kepler* space telescope, based on data obtained over nearly 2.5 yr. All four stars are found to be multiperiodic. The strongest secondary mode with frequency f_2 has an amplitude of a few mmag, 20–45 times lower than the main radial mode with frequency f_1. The two oscillations have a period ratio of $P_2/P_1 = 0.612$–0.632 that cannot be reproduced by any two radial modes. Thus, the secondary mode is non-radial. Modes yielding similar period ratios have also recently been discovered in other variables of the RRc and RRd types. These objects form a homogenous group and constitute a new class of multimode RR Lyrae pulsators, analogous to a similar class of multimode classical Cepheids in the Magellanic Clouds. Because a secondary mode with $P_2/P_1 \sim 0.61$ is found in almost every RRc and RRd star observed from space, this form of multiperiodicity must be common. In all four *Kepler* RRc stars studied, we find subharmonics of f_2 at $\sim 1/2 f_2$ and at $\sim 3/2 f_2$. This is a signature of period doubling of the secondary oscillation, and is the first detection of period doubling in RRc stars. The amplitudes and phases of f_2 and its subharmonics are variable on a time-scale of 10–200 d. The dominant radial mode also shows variations on the same time-scale, but with much smaller amplitude. In three *Kepler* RRc stars we detect additional periodicities, with amplitudes below 1 mmag, that must correspond to non-radial g-modes. Such modes never before have been observed in RR Lyrae variables.

Key words: techniques: photometric – stars: horizontal branch – stars: oscillations – stars: variables: RR Lyrae.

1 INTRODUCTION

RR Lyrae variables are evolved stars burning helium in their cores. In the Hertzsprung–Russell diagram they are located at the intersection of the horizontal branch and the classical instability strip, in

⋆ E-mail: pam@camk.edu.pl

which the κ-mechanism operating in the H and He partial ionization zones drives the pulsation. They are classified according to their pulsation characteristics using a variant of the initial classification by Bailey (1902). The subclass of the RRab stars is by far the largest. These stars pulsate in the radial fundamental mode (F), with periods of 0.3–1.0 d, and peak-to-peak amplitudes in V ranging from few tenths of magnitude at long periods to more than 1 mag at short periods. Their light curves are asymmetric (steeper on the rising part). Their less numerous siblings are the RRc stars, which pulsate in the first overtone radial mode (1O) with shorter periods in the range 0.2–0.5 d, and with more sinusoidal light curves with lower amplitudes of about 0.5 mag in V, peak to peak. Even less numerous are the RRd stars, which pulsate simultaneously in the radial first overtone mode and the radial fundamental mode (F+1O).

Playing an important role in distance determination and in Galactic structure and evolution studies, RR Lyrae stars are among the best studied and most observed classes of variable stars. In recent years, dozens of RR Lyrae stars have been observed with unprecedented precision from space by the *MOST* (Gruberbauer et al. 2007), *CoRoT* (e.g. Szabó et al. 2014) and *Kepler* (e.g. Benkő et al. 2010; Kolenberg et al. 2010) telescopes.

Nevertheless, many intriguing puzzles surround the RR Lyrae stars. The most stubborn problem is the Blazhko effect, a quasi-periodic modulation of pulsation amplitude and phase that has been known for more than 100 yr (Blazhko 1907). Dedicated ground-based campaigns (Jurcsik et al. 2009) and results of *Kepler* observations (Benkő et al. 2010) indicate that up to 50 per cent of the RRab stars show Blazhko modulation. For the RRc stars the incidence rate is probably lower. Ground-based observations show it is below 10 per cent (e.g. Mizerski 2003; Nagy & Kovács 2006). We lack high-precision space observations for these stars. Only recently the first Blazhko modulated RRc star was observed from space by *Kepler* (Molnár et al., in preparation) . Despite many important discoveries, including detection of period doubling (Szabó et al. 2010) and of excitation of additional radial modes in Blazhko variables (Benkő et al. 2010, 2014; Molnár et al. 2012) our understanding of the Blazhko effect remains poor (for a review see Szabó 2014).

Another mystery is the mode selection process in RR Lyrae stars: we do not know why some stars pulsate in two radial modes simultaneously. The ability of current non-linear pulsation codes to model this form of pulsation is still a matter of debate; see, e.g. Kolláth et al. (2002) and Smolec & Moskalik (2008b) for opposing views. Recent discoveries of F+2O radial double-mode pulsations and the detection of non-radial modes in RR Lyrae stars (see Moskalik 2013, 2014 for reviews) make the mode-selection problem even more topical and puzzling. Particularly interesting is the excitation of non-radial modes, evidence of which is found in all subclasses of RR Lyrae variables. Their presence seems to be a frequent phenomenon in these stars.

This paper describes new properties of first overtone RR Lyrae stars, some of them revealed for the first time by the high-precision *Kepler* photometry. We present an in-depth study of four RRc stars in the *Kepler* field: KIC 4064484, KIC 5520878, KIC 8832417 and KIC 9453114. Partial results of our analysis have been published in Moskalik et al. (2013). They have also been included in a review paper of Moskalik (2014). Here we present a full and comprehensive discussion of the results.

In Section 2, we describe the *Kepler* photometry and our methods of data reduction. Properties of the four RRc variables are summarized in Section 3. Our main findings are discussed in Sections 4–6, where we present the results of frequency analyses of the stars and describe amplitude and phase variability of the detected pulsation modes. In Section 7, we put the *Kepler* RRc stars in a broader context of other recently identified multimode RRc variables and discuss the group properties of this new type of multimode pulsators. Our conclusions are summarized in Section 8.

2 *KEPLER* PHOTOMETRY

The *Kepler* space telescope was launched on 2009 March 6 and placed in a 372.5-d Earth trailing heliocentric orbit. The primary purpose of the mission was to detect transits of Earth-size planets orbiting Sun-like stars (Borucki et al. 2010). This goal was achieved[1] by nearly continuous, ultraprecise photometric monitoring of nearly 200 000 stars in the 115 deg^2 field of view. A detailed description of the mission design and its in-flight performance is presented in Koch et al. (2010), Caldwell et al. (2010), Haas et al. (2010), Jenkins et al. (2010a,b) and Gilliland et al. (2010). *Kepler*'s primary mission ended after four years when the second reaction wheel failed in 2013 May.

The *Kepler* magnitude system (*Kp*) corresponds to a broad spectral bandpass, from 423 nm to 897 nm. The time series photometric data delivered by the *Kepler* telescope come in two different formats: long cadence (LC) and short cadence (SC), with sampling rates of 29.43 min and 58.86 s, respectively. The time of mid-point of each measurement is corrected to Barycentric Julian Date (BJD). Four times per orbital period the spacecraft was rotated by 90° to keep optimal illumination of its solar arrays. These rolls naturally organize the data into quarters, denominated Q1, Q2, etc, where each quarter lasts about three months (except the first and the last quarter, which are shorter). The data are almost continuous, with only small gaps due to regular data downlink periods and to infrequent technical problems (safe mode, loss of pointing accuracy). The typical duty cycle of the *Kepler* light curve is 92 per cent.

2.1 Data reduction

The *Kepler* telescope is equipped with 42 science CCDs (Koch et al. 2010). A given star fell on four different CCDs with each quarterly roll of the spacecraft, then returned to the original CCD. As a result of different sensitivity levels, the measured flux jumps from quarter to quarter. For some stars slow trends also occur within each quarter, due to image motion, secular focus changes or varying sensitivity of the detector (Jenkins et al. 2010a). All these instrumental effects need to be corrected before starting the data analysis.

Our data reduction procedure is similar to that of Nemec et al. (2011). We use the 'raw' fluxes, properly called Simple Aperture Photometry fluxes (Jenkins et al. 2010a). The detrending is done separately for each quarter. The flux time series is first converted into a magnitude scale. Slow drifts in the magnitudes are then removed by subtracting a polynomial fit. Next, the data are fitted with the Fourier sum representing a complete frequency solution. The residuals of this fit are inspected for any additional low-level drifts, which are again fitted with a polynomial and subtracted from the original magnitudes (secondary detrending). The detrended data for each quarter are then shifted to the same average magnitude level. As the final step, all quarters are merged, forming a quasi-continuous *Kp* magnitude light curve of a star. An example of a reduced light curve is displayed in Fig. 1.

[1] http://kepler.nasa.gov/Mission/discoveries/candidates/

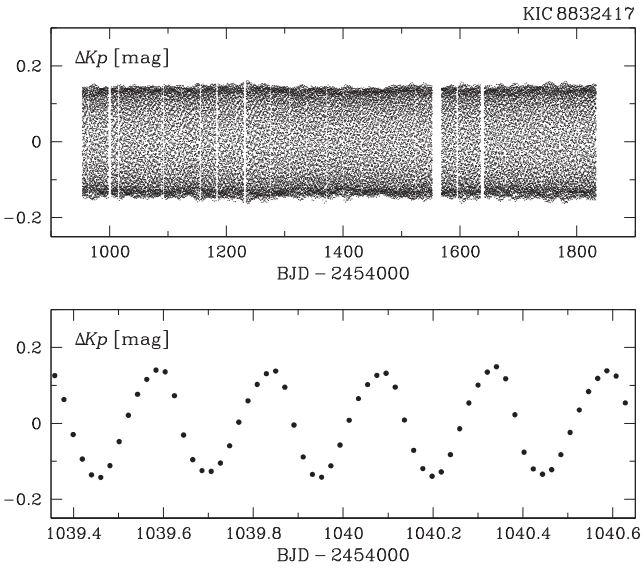

Figure 1. *Kepler* light curve of RRc stars KIC 8832417 for Q0 − Q10. Upper panel: entire light curve. Bottom panel: short segment of the light curve.

3 RRC STARS IN THE *KEPLER* FIELD

More than 50 RR Lyrae variables are currently identified in the *Kepler* field (Kolenberg et al. 2014). At the time this study was initiated, only four of them were classified as RRc pulsators. Basic characteristics of these four stars are given in Table 1. The first four columns of the table list the star numbers, equatorial sky coordinates (α, δ) and mean *Kp* magnitude, all taken from the *Kepler* Input Catalogue (KIC, Brown et al. 2011) . Columns 5 and 6 contain the pulsation periods and the total (peak-to-peak) amplitudes. All four RRc stars turned out to be multiperiodic (Section 4), but they are all strongly dominated by a single radial mode. The periods and amplitudes given in the table correspond to this dominant mode of pulsation. They are determined from the *Kepler* light curves. Column 7 contains spectroscopic metal abundances, [Fe/H], from Nemec et al. (2013). Two stars in our RRc sample are metal-rich (KIC 5520878 and KIC 8832417), the other two are metal-poor. Column 8 indicates other identifications of the stars. KIC 9453114 is also known as ROTSE1 J190350.47+460144.8. None of the *Kepler* RRc variables has a GCVS name yet.

The last column of Table 1 lists *Kepler* observing runs analysed in this paper. Here, we use only the LC photometry, collected in quarters Q1 to Q10. For KIC 8832417 and KIC 9453114 it is supplemented by 10 d of commissioning data (Q0). Due to the loss of CCD module no. 3, no photometry was obtained for KIC 4064484 in Q6 and Q10. The total time base of the data ranges from 774 d for KIC 4064484 to 880 d for KIC 8832417 and KIC 9453114.

Fig. 2 displays phased light curves of the dominant mode of *Kepler* RRc stars. The plot is constructed with Q0+Q1 data, which

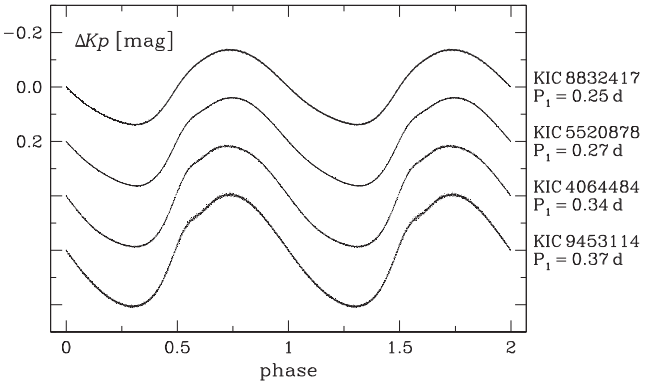

Figure 2. Phased light curves of the dominant radial mode of *Kepler* RRc stars.

Table 2. Light curve shape parameters for the dominant radial mode of *Kepler* RRc stars. Values are determined from Q0+Q1 data.

KIC	$\log P_1$ (d)	A_1 (mmag)	R_{21}	ϕ_{21} (rad)	$M-m$
8832417	− 0.605	138.40	0.1015	4.661	0.425
5520878	− 0.570	162.88	0.1078	4.704	0.427
4064484	− 0.472	190.50	0.1109	4.813	0.408
9453114	− 0.436	206.38	0.0982	4.828	0.430

were pre-whitened by all frequencies other than the dominant one ($f_1 = 1/P_1$) and its harmonics (Section 4). The light curves are typical for radial first overtone pulsators, with round tops, long rise times and low amplitudes. The change of slope which occurs shortly before the brightness maximum is also characteristic for the RRc variables (e.g. Lub 1977; Olech et al. 2001).

To describe light curve shape in a quantitative way, we resort to a Fourier decomposition (Simon & Lee 1981). We fit the light curves of Fig. 2 with the Fourier sum of the form

$$Kp(t) = A_0 + \sum_k A_k \cos(2\pi k f_1 t + \phi_k), \quad (1)$$

and then compute the usual Fourier parameters: the amplitude ratio $R_{21} = A_2/A_1$ and the phase difference $\phi_{21} = \phi_2 - 2\phi_1$. They are listed in Table 2, together with the semi-amplitude of the dominant frequency, A_1 ($\approx A_{\rm tot}/2$). The last column of the table gives another light curve parameter: the interval from minimum to maximum, expressed as a fraction of the pulsation period. This quantity measures asymmetry of the light curve and is traditionally called $M-m$ (Payne-Gaposchkin & Gaposchkin 1966) or a risetime parameter (e.g. Nemec et al. 2011). For all four variables in Table 2 this parameter is above 0.4, which agrees with their classification as RRc stars (Tsesevich 1975).

In Fig. 3, we compare the Fourier parameters and the peak-to-peak amplitudes $A_{\rm tot}$ of the *Kepler* RRc stars with those of RR

Table 1. RRc stars in the *Kepler* field. Periods and amplitudes are determined from Q0+Q1 long-cadence data.

KIC ID	α (J 2000)	δ (J 2000)	$\langle Kp\rangle$ (mag)	Period (d)	$A_{\rm tot}(Kp)$ (mag)	[Fe/H]	Name	Data
4064484	19 33 45.49	+ 39 07 14.00	14.641	0.3370019	0.371	− 1.58		Q1 − Q5, Q7 − Q9
5520878	19 10 23.58	+ 40 46 04.50	14.214	0.2691699	0.324	− 0.18	ASAS 191024+4046.1	Q1 − Q10
8832417	19 46 54.31	+ 45 04 50.23	13.051	0.2485464	0.275	− 0.27	ASAS 194654+4504.8	Q0 − Q10
9453114	19 03 50.52	+ 46 01 44.11	13.419	0.3660786	0.410	− 2.13	ASAS 190350+4601.7	Q0 − Q10

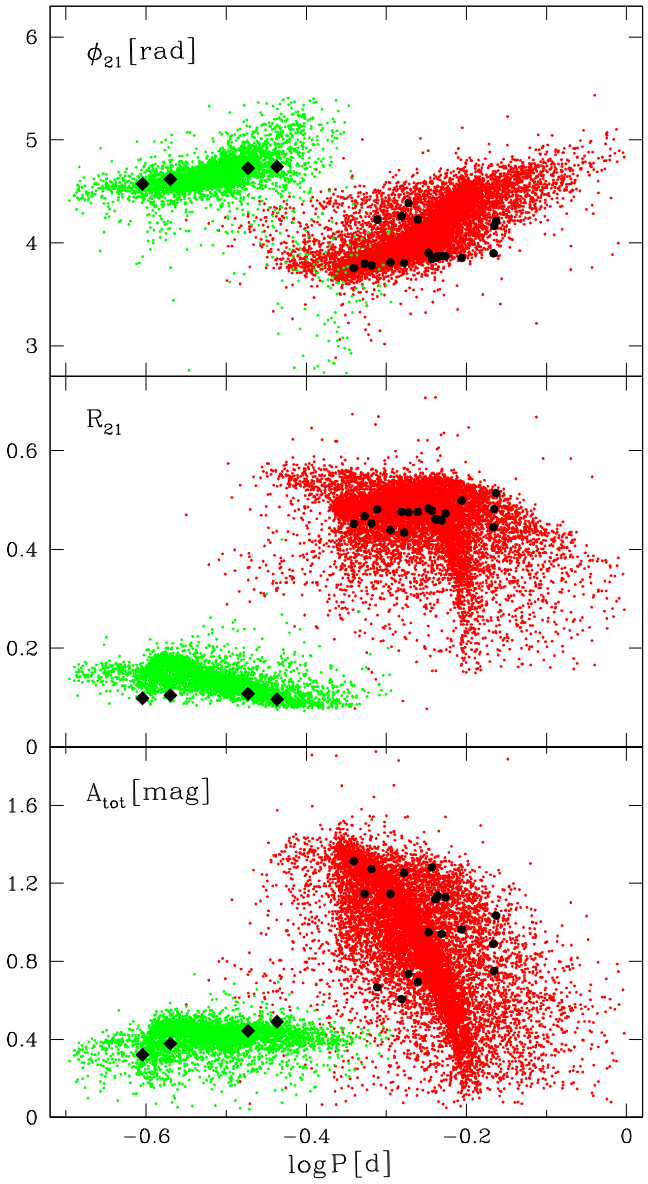

Figure 3. Fourier parameters (V band) of *Kepler* RRc stars (black diamonds) and non-Blazhko RRab stars (black circles). The Galactic Bulge RR Lyrae stars (Soszyński et al. 2011a) are displayed for comparison, with the first overtone (RRc) and the fundamental mode (RRab) variables plotted as green and red dots, respectively.

Lyrae stars in the Galactic Bulge (Soszyński et al. 2011a). *Kepler* non-Blazhko RRab stars (Nemec et al. 2011) are also displayed. All parameters are converted to a common photometric band, namely to Johnson V. For the Bulge variables, R_{21} and ϕ_{21} are transformed from I to V with the formula of Morgan, Simet & Bargenquast (1998). For the amplitude, we use equation $A_{\rm tot}(V) = 1.62A_{\rm tot}(I)$, derived by us from photometry of RR Lyrae stars in M68 (Walker 1994). The amplitude transformation is the same for RRab and for RRc stars. In case of the *Kepler* variables, ϕ_{21} is transformed from Kp to V according to equation 2 of Nemec et al. (2011), but for $A_{\rm tot}$ and R_{21} we used proportional scaling, which in our opinion is more appropriate. Using the same data as Nemec et al. (2011), we derive $A_{\rm tot}(V) = 1.16A_{\rm tot}(Kp)$ and $R_{21}(V) = 0.975R_{21}(Kp)$.

All $Kp \rightarrow V$ transformation formulae are calibrated with RRab stars, thus applying them to the RRc stars can yield only approximate results. This approximation is still sufficiently accurate, particularly for $A_{\rm tot}$ (where scaling is mode-independent) and for ϕ_{21} (where colour-to-colour corrections are always small). We expect the approximation to be least accurate in the case of R_{21}, for which colour-to-colour scaling is somewhat dependent on the pulsation mode (Morgan et al. 1998).

Fig. 3 shows that the Fourier parameters of variables listed in Table 1 (black diamonds) are very different from those of the *Kepler* RRab stars. At the same time, they match typical values for the first overtone RR Lyrae stars well. The figure proves that the variables of Table 1 belong to the population of RRc stars.

4 DATA ANALYSIS AND RESULTS

We analysed the pulsations of *Kepler* RRc stars with a standard Fourier transform (FT) combined with the multifrequency least-squares fits and consecutive pre-whitening. We used well-tested software written by Z. Kołaczkowski (see Moskalik & Kołaczkowski 2009). The light curve was first fitted with a Fourier series representing variations with the dominant frequency, f_1 (equation 1). After subtracting the fitted function (pre-whitening), the residuals were searched for secondary periods. This was done with the FT, computed over the range from 0 to 24.5 $\rm d^{-1}$, which is the Nyquist frequency of the LC data. Newly identified frequencies were included into the Fourier series, which was fitted to the light curve again. The residuals of the fit were searched for more frequencies. The whole procedure was repeated until no new periodicities were found. In each step, all frequencies were optimized by the least-squares routine. The final fit yields frequencies, amplitudes and phases of all identified harmonic components.

All four *Kepler* RRc variables turned out to be multiperiodic. Very early in the analysis, we realized that the amplitudes and phases of the detected frequencies are not constant. Therefore, we first discuss only a short segment of available data, namely Q0+Q1. Our goal here is to establish the frequency content of the RRc light curves. We defer the analysis of the entire Q0 – Q10 data sets and discussion of temporal behaviour of the modes to Section 5. In the following subsections, we present the results for each of the investigated RRc stars individually. We discuss the stars in order of decreasing amplitude stability, which nearly coincides with the order of increasing pulsation period.

4.1 KIC 5520878

Fig. 4 shows the pre-whitening sequence for KIC 5520878. The FT of its light curve (upper panel) is strongly dominated by the radial mode with frequency $f_1 = 3.715126$ $\rm d^{-1}$ and amplitude $A_1 = 162.88$ mmag. After subtracting f_1 and its harmonics from the data, the FT of the residuals (middle panel) shows the strongest peak at $f_2 = 5.878\,58$ $\rm d^{-1}$. This secondary mode has an amplitude of only $A_2 = 7.04$ mmag, 23 times lower than A_1. Its harmonic and several combinations with f_1 are also clearly visible. The period ratio of the two modes is $P_2/P_1 = 0.6320$. After pre-whitening the light curve with both f_1, f_2 and their harmonics and combinations (bottom panel), the strongest remaining signal appears at $f_3 = 2.936\,94$ $\rm d^{-1}$, i.e. at $\sim 1/2f_2$. Thus, f_3 is not an independent frequency, it is a *subharmonic* of f_2. A second subharmonic at $f_{3'} = 8.814\,28$ $\rm d^{-1} \sim 3/2f_2$ is also present. The remaining peaks in the FT correspond to linear combinations of f_1 with f_3 and $f_{3'}$. In Table 3, we list all harmonics, subharmonics and combination frequencies identified in Q1 light curve of KIC 5520878.

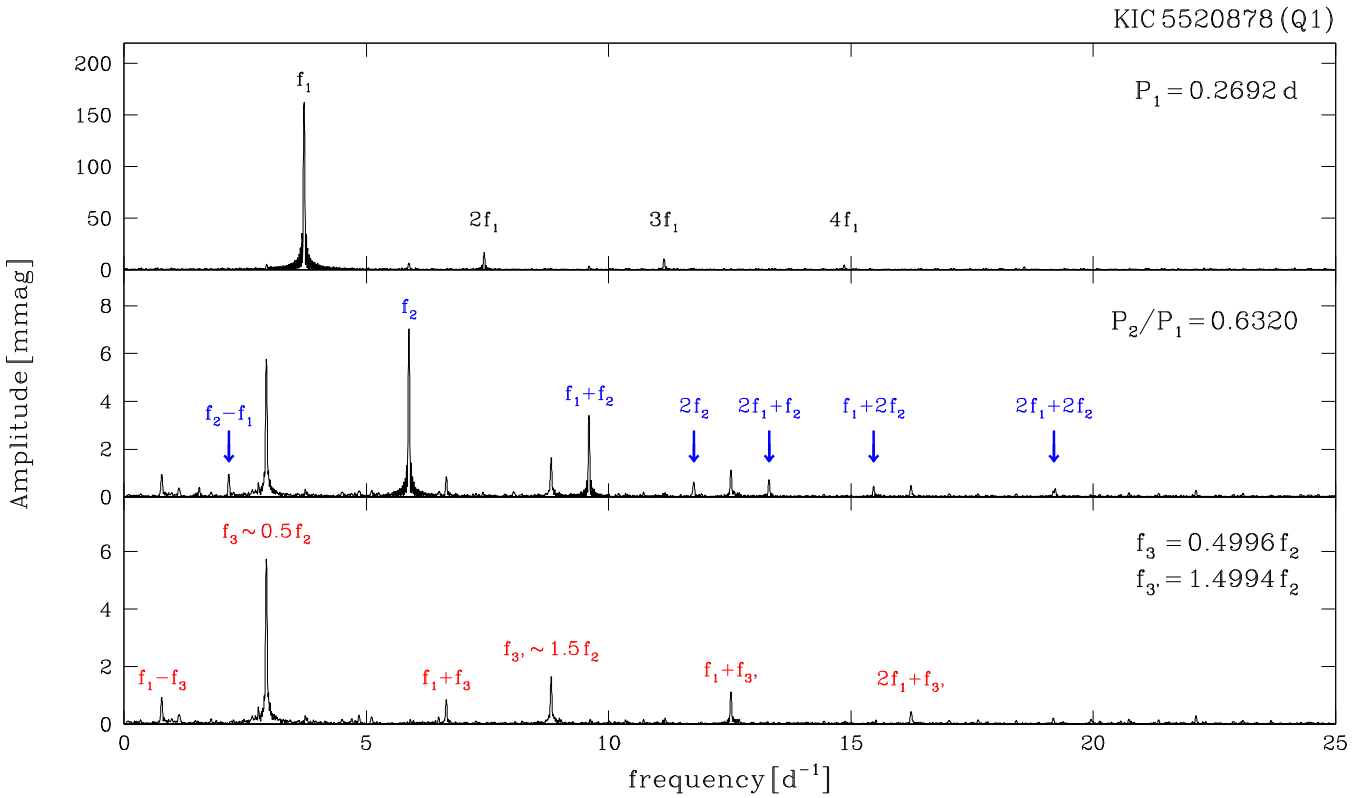

Figure 4. Pre-whitening sequence for KIC 5520878. The upper panel displays the FT of the original *Kp* magnitude light curve. The middle and bottom panels show FTs after consecutive pre-whitening steps (see text). Only Q1 data are analysed here.

Table 3. Main frequency components identified in Q1 light curve of KIC 5520878.

Frequency	f (d^{-1})	A (mmag)	Frequency	f (d^{-1})	A (mmag)	Frequency	f (d^{-1})	A (mmag)
f_1	3.715 126	162.88	$f_1 - f_2$	2.160 17	0.95	$0.5f_2$	2.936 94	5.74
$2f_1$	7.430 253	17.55	$2f_1 - f_2$	1.551 80	0.41	$1.5f_2$	8.814 28	1.65
$3f_1$	11.145 379	11.06	$f_1 + f_2$	9.596 25	3.37	$f_1 - 0.5f_2$	0.779 49	0.95
$4f_1$	14.860 506	4.77	$2f_1 + f_2$	13.310 87	0.76	$2f_1 - 0.5f_2$	4.486 80	0.18:
$5f_1$	18.575 632	2.61	$3f_1 + f_2$	17.025 11	0.16:	$f_1 + 0.5f_2$	6.649 48	0.87
$6f_1$	22.290 759	1.39	$4f_1 + f_2$	20.739 73	0.16:	$f_1 - 1.5f_2$	5.105 93	0.26
$7f_1$	26.005 885	0.78	$f_1 - 2f_2$	8.038 27	0.26	$f_1 + 1.5f_2$	12.525 31	1.13
$8f_1$	29.721 011	0.37	$f_1 + 2f_2$	15.468 26	0.44	$2f_1 + 1.5f_2$	16.242 51	0.44
f_2	5.878 58	7.04	$2f_1 + 2f_2$	19.180 85	0.18:	$3f_1 + 1.5f_2$	19.955 92	0.16:
$2f_2$	11.758 77	0.65	$f_1 + 3f_2$	21.350 66	0.14:	$f_1 + 2.5f_2$	18.410 40	0.14:
$3f_2$	17.625 23	0.13:				$2f_1 + 2.5f_2$	22.124 52	0.29

4.2 KIC 8832417

Pulsations of this star are dominated by the radial mode with frequency $f_1 = 4.023\,39$ d^{-1}. After pre-whitening the data with f_1 and its harmonics (Fig. 5, second panel), we identify a secondary mode at $f_2 = 6.572\,03$ d^{-1}. The resulting period ratio is $P_2/P_1 = 0.6122$. The subharmonic of the secondary frequency at $\sim 3/2f_2$ is clearly visible. The subharmonic at $\sim 1/2f_2$ is present as well, but its appearance is different. The peak is very broad and almost split into three close components. Such a pattern implies that we look either at a group of frequencies that are too close to be resolved, or at a single frequency with unstable amplitude and/or phase. The central component of this subharmonic power is located at $f_3 = 3.298\,48$ d^{-1} $= 0.5019f_2$. The remaining peaks in the pre-whitened FT correspond to linear combinations of f_1 with f_2 and $3/2f_2$.

4.3 KIC 4064484

Pulsations of KIC 4064484 are dominated by the radial mode with frequency $f_1 = 2.967\,34$ d^{-1}. After pre-whitening the data with f_1 and its harmonics (Fig. 5, third panel), we find a secondary mode at $f_2 = 4.82044$ d^{-1}, yielding a period ratio of $P_2/P_1 = 0.6156$. The peak corresponding to f_2 is broadened and starts to split into several unresolved components. The same is true for the combination peaks at $f_2 - f_1$, $f_1 + f_2$, $2f_1 + f_2$, etc. As in the other two RRc stars, we find a subharmonic of the secondary frequency at $\sim 3/2f_2$. This peak is also broadened and split, and so are the corresponding combination peaks. Unlike the previous two RRc stars, in KIC 4064484 we do not detect a clear subharmonic at $\sim 1/2f_2$. There is an excess of power in the vicinity of this frequency, but it forms a dense forest of peaks, none of which stand out.

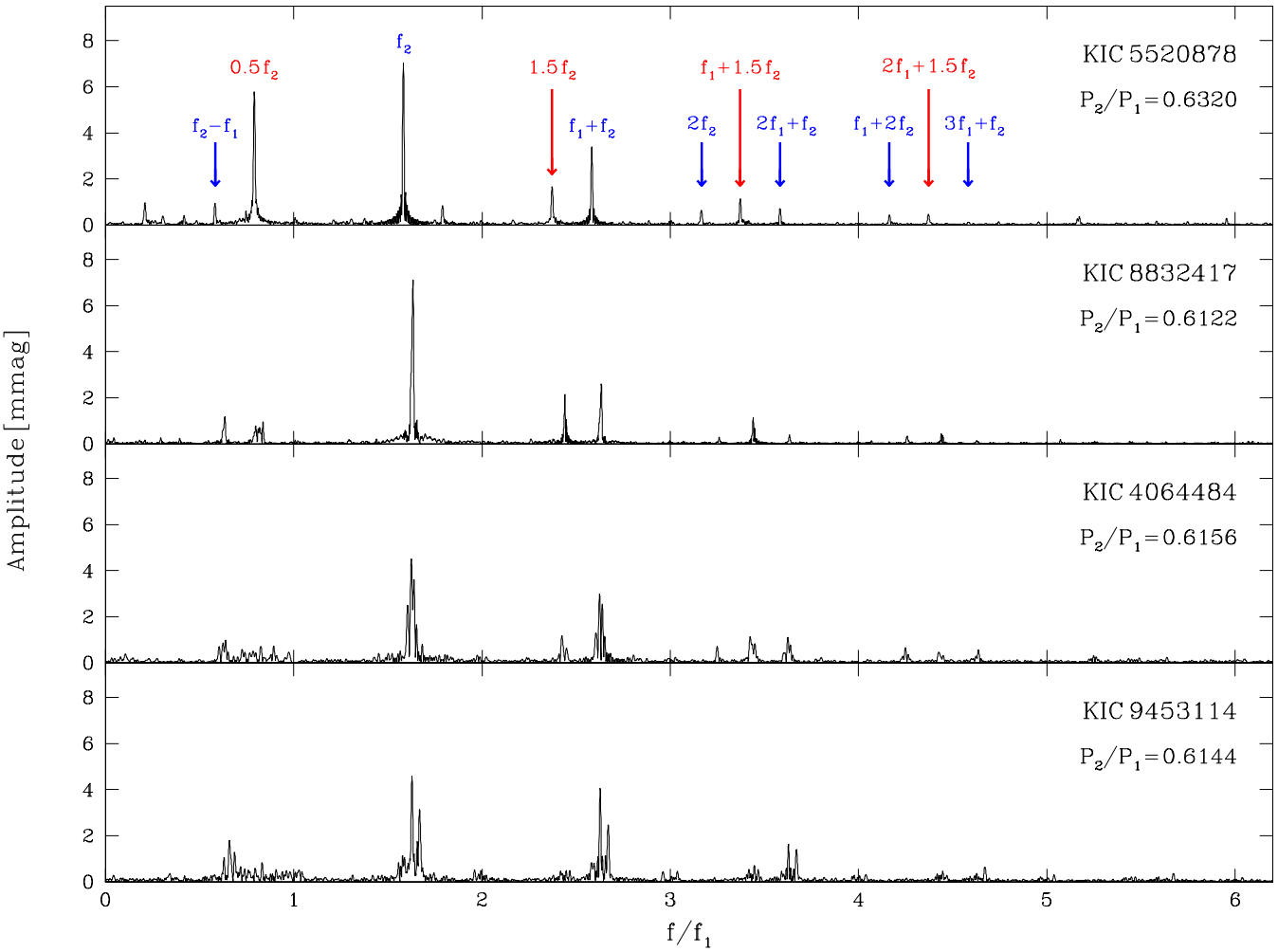

Figure 5. Frequency spectra of the four *Kepler* RRc stars (Q0+Q1 data only) after pre-whitening by f_1 and its harmonics. FT of KIC 5520878 (upper panel) is the same as plotted in the middle panel of Fig. 4.

4.4 KIC 9453114

The dominant radial mode of KIC 9453114 has a frequency of $f_1 = 2.731\,64$ d^{-1}. After pre-whitening the light curve with f_1 and its harmonics (Fig. 5, bottom panel), we find a secondary mode at $f_2 = 4.446\,43$ d^{-1}, yielding a period ratio of $P_2/P_1 = 0.6143$. A second peak of somewhat lower amplitude is present next to it, at $f_{2'} = 4.558\,30$ d^{-1}. Another much weaker peak can be identified at the same distance from f_2, but on its opposite side. Thus, the secondary frequency in KIC 9453114 is split into three *resolved components*, which form an approximately equidistant triplet. The same pattern is also seen at the combination frequencies $f_2 - f_1$, $f_1 + f_2$, $2f_1 + f_2$, etc. The f_2 triplet can be interpreted in two physically different ways: either as a multiplet of non-radial modes ($\ell \geq 1$) split by rotation or as a single mode undergoing a periodic or quasi-periodic modulation. A close inspection of the triplet shows that all three components are incoherent. Indeed, an attempt to pre-whiten them with three sine waves of constant amplitudes and phases proves unsuccessful, leaving significant residual power. This casts doubt on the non-radial multiplet interpretation. We will return to this point in Section 5.1.2.

Although very weak, the subharmonics of f_2 are also present in KIC 9453114. The signal corresponding to $\sim 3/2f_2$ is detected at $f_{3'} = 6.684\,87$ d^{-1}. Its combination frequencies at $\sim f_1 + f_{3'}$ and $\sim 2f_1 + f_{3'}$ can be identified, too. All these peaks are split into resolved triplets. A second subharmonic ($\sim 1/2f_2$) is detected as well, as a marginally significant single peak at $f_3 = 2.273\,40$ d^{-1}.

4.5 Similarity of *Kepler* RRc stars

The results of the frequency analyses of *Kepler* RRc variables are summarized in Table 4. In Fig. 5, we display the FTs of their Q0+Q1 light curves, pre-whitened of the dominant radial mode. For better comparison, the FTs are plotted versus normalized frequency, f/f_1.

All four RRc variables are multiperiodic. Fig. 5 shows that their frequency spectra are remarkably similar and display peaks at the same places. In each star we detect a secondary mode, which appears at $f_2/f_1 = 1.58$–1.63 or $P_2/P_1 = 0.612$–0.632. This is always the highest secondary peak, yet its amplitude is only a few mmag and is 20–45 times lower than the amplitude of the radial mode. Without the benefit of the high-precision *Kepler* photometry, such a weak signal is very difficult to detect.

In each variable, we identify at least one subharmonic of the secondary frequency. The signal at $\sim 3/2f_2$ is detected in all *Kepler* RRc stars. The second subharmonic at $\sim 1/2f_2$ is visible in three of the stars, although it is prominent only in KIC 5520878. The presence of subharmonics, i.e. frequencies of the form $(n + 1/2)f$,

Table 4. Primary and secondary periodicities in *Kepler* RRc stars, determined from Q0+Q1 data.

KIC	P_1 (d)	A_1 (mmag)	P_2 (d)	A_2 (mmag)	$P_{3,3'}$ (d)	$A_{3,3'}$ (mmag)	P_2/P_1	$f_{3,3'}/f_2$
8832417	0.248 5464	138.40	0.152 16	7.11	0.303 17	0.69	0.612 18	0.5019
					0.101 86	2.14		1.4937
5520878	0.269 1699	162.88	0.170 11	7.04	0.340 49	5.74	0.631 97	0.4996
					0.113 45	1.65		1.4994
4064484	0.337 0019	190.50	0.207 45	4.55	0.139 01	1.21	0.615 58	1.4923
9453114	0.366 0809	206.64	0.224 90	4.55	(0.439 87)	(0.81)	0.614 35	(0.5113)
					0.149 59	0.46		1.5034

is a characteristic signature of a period doubling (Bergé, Pomeau & Vidal 1986; see also fig. 3 of Smolec & Moskalik 2012). Thus, our finding constitutes the first detection of the period doubling phenomenon in the RRc variables (see also Moskalik et al. 2013; Moskalik 2014). These stars are thus the fourth class of pulsators in which period doubling has been discovered, following the RV Tauri stars (known for decades), and the Blazhko RRab stars (Kolenberg et al. 2010; Szabó et al. 2010) and the BL Herculis stars (Smolec et al. 2012), only identified recently.

We note, that the subharmonics listed in Table 4 are never located at precisely $1/2f_2$ and $3/2f_2$. The deviations from the exact half-integer frequency ratios are very small, almost never exceeding 0.5 per cent, but they are statistically significant. We recall, that similar deviations are also observed for period doubling subharmonics in the Blazhko RRab stars (Szabó et al. 2010, 2014; Kolenberg et al. 2011; Guggenberger et al. 2012). This behaviour has been traced to the non-stationary character of the subharmonics, which causes their instantaneous frequencies to fluctuate around the expected values (Szabó et al. 2010). The same reasoning applies also to the RRc stars. As we will discuss in the next section, the subharmonics detected in these variables are non-stationary as well.

Finally, we note that a secondary mode with $P_2/P_1 \sim 0.61$ and its subharmonics are detected in *every* RRc star observed by *Kepler*. This suggests that excitation of this mode and the concomitant period doubling is not an exception, but is a common property of the RRc variables. We return to this point in Section 7.

5 VARIABILITY OF AMPLITUDES AND PHASES

5.1 f_2 and its subharmonics

We start the discussion with the secondary mode, f_2, for which evidence of instability is most noticeable. Fig. 5 presents RRc frequency spectra computed for month-long subsets of available data. Already for this short timebase, the Fourier peaks corresponding to f_2 and its subharmonics are broadened or even split. This indicates that amplitudes and/or phases of these frequency components are variable. To examine this variability in detail, in this section we analyse for each star the entire light curve, covering quarters Q0 – Q10.

5.1.1 Time domain

We examine the temporal behaviour of modes by applying a time-dependent Fourier analysis (Kovács, Buchler & Davis 1987). To this end, we subdivide the light curve into short overlapping segments with duration Δt, and then fit a Fourier series consisting of all significant frequency terms to each segment separately.

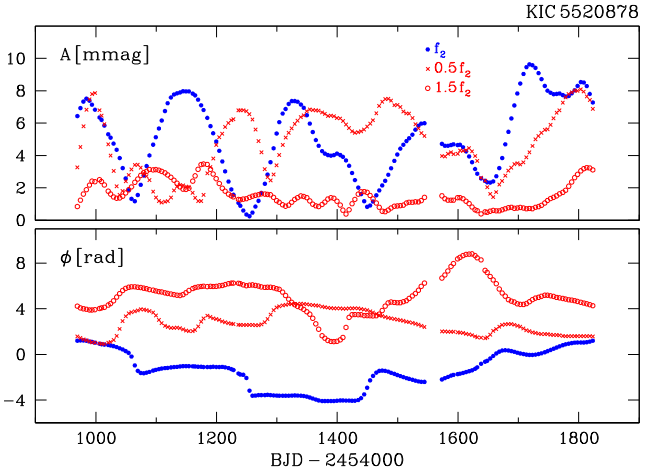

Figure 6. Variability of the secondary mode and its subharmonics in KIC 5520878. Upper panel: amplitude variations. Bottom panel: phase variations.

All frequencies are kept fixed. The choice of Δt is somewhat arbitrary and depends on how fast the amplitudes and phases change. With this procedure, we can follow the temporal evolution of all frequency components present in the data.

In Fig. 6, we present results of such an analysis for KIC 5520878. For this star we adopted $\Delta t = 10$ d. The plot displays amplitudes and phases of the secondary mode, f_2, and of its two subharmonics, $1/2f_2$ and $3/2f_2$. The amplitude of the secondary mode varies in a rather irregular fashion, with a time-scale of ∼200 d. The range of these variations is extremely large: from almost 0 to 9.6 mmag. In other words, the amplitude of f_2 fluctuates by nearly 100 per cent! Both subharmonics of f_2 display large, irregular changes as well. Interestingly, although occurring with approximately the same time-scale, they do not seem to be correlated with variations of the parent mode – the maximum (minimum) amplitudes of the subharmonics in some instances coincide with maximum (minimum) amplitude of f_2, but in other instances they do not. The amplitude variability of the secondary mode and its subharmonic is accompanied by irregular variability of their phases (Fig. 6, bottom panel).

In Fig. 7, we compare amplitude variability of all four *Kepler* RRc stars. Only 150 d of data is displayed. For the consecutive objects (top to bottom), we adopted $\Delta t = 10$ d, 5 d, 5 d and 3 d, respectively. Strong amplitude variations of secondary periodicities are found in all the stars. These variations are always irregular. As such, they are *not compatible with beating* of two or more stable modes. The time-scale of amplitude changes is not the same in every RRc variable. It ranges from ∼200 d (KIC 5520878) to ∼10 d (KIC 9453114) and becomes progressively shorter as we go from shorter to longer

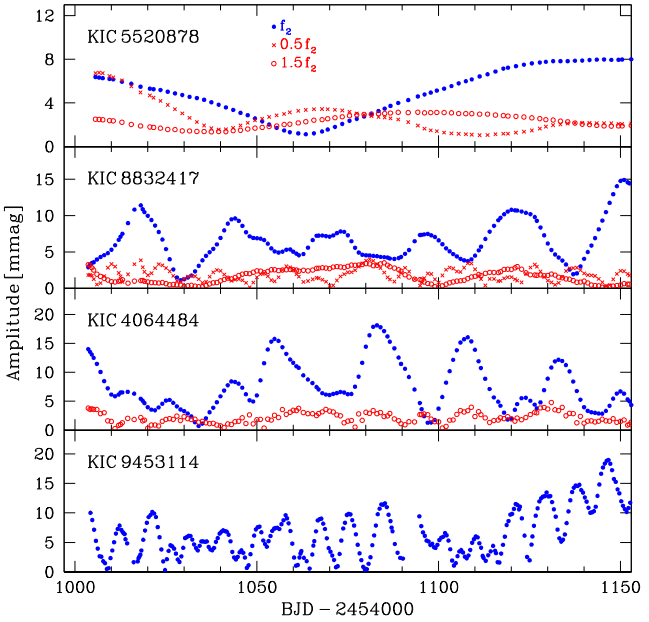

Figure 7. Amplitude variations of the secondary mode and its subharmonics in *Kepler* RRc stars. For better visibility, amplitudes of subharmonics in KIC 8832417 (KIC 4064484) are multiplied by 1.5 (by 2.0). Subharmonics of KIC 9453114 are too weak to be securely extracted from short segments of data. Only part of total data is displayed.

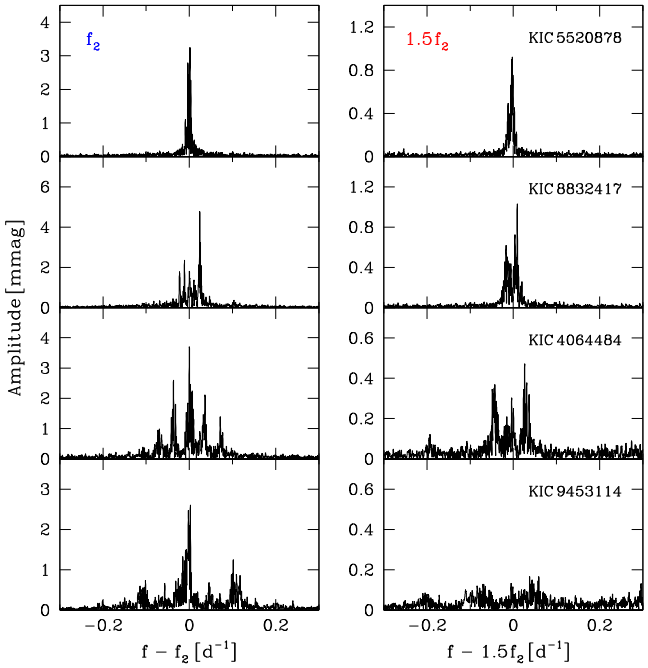

Figure 8. Pre-whitened frequency spectra of *Kepler* RRc stars, computed for the entire light curves (Q0 − Q10). Left-hand column: FT of the secondary mode, f_2. Right-hand column: FT of its subharmonic at $3/2f_2$.

period pulsators. This tendency explains why Fourier peaks in Fig. 5 become broader with the increasing pulsation period of the star.

As in the case of KIC 5520878, secondary periodicities in all RRc stars display significant phase variations (not shown). They occur on the same time-scale as the variations of the respective amplitudes. We recall here that a phase change of a mode is equivalent to a change of its frequency. Indeed, the difference between the instantaneous and the mean frequency is

$$\Delta\omega = 2\pi\Delta f = \frac{\mathrm{d}\phi}{\mathrm{d}t}. \qquad (2)$$

Thus, the frequencies of the secondary mode and its subharmonics are not constant in *Kepler* RRc stars, but fluctuate on a time-scale of 10–200 d. This is the reason why the values of f_3/f_2 and $f_{3'}/f_2$ (see Table 4) deviate from the exact half-integer ratios. These deviations are larger in stars in which phase variations are faster.

5.1.2 *Frequency domain*

For each studied RRc star, we computed the FT of the entire light curve (Q0 − Q10), after pre-whitening it with the dominant (radial) frequency and its harmonics. The resulting frequency patterns in the vicinity of the secondary mode, f_2, and its subharmonic, $3/2f_2$, are displayed in Fig. 8.

Because the secondary mode in RRc stars has variable amplitude and phase, it cannot be represented in the FT by a single sharp peak. Fig. 8 confirms this. In the case of KIC 5520878, f_2 is visibly broadened, but still does not split into resolved components. For the other three stars, the mode splits into a quintuplet of well-separated, equally-spaced peaks (see also Fig. 12). Such a pattern suggests that f_2 might correspond to a multiplet of $\ell = 2$ non-radial modes. However, this is not the only possible interpretation.

We notice that each component of the quintuplet is broadened and in fact forms a band of power. None of them can be attributed to a stable mode with a well-defined amplitude and frequency. We can interpret this in two different ways. The f_2 frequency pattern might be explained as a rotationally split multiplet of non-radial modes, of the same ℓ and different m, all of which are non-stationary. Alternatively, the observed pattern might result from a quasi-periodic modulation of a single mode. In the latter picture, the existence of a quasi-period is responsible for splitting f_2 into well-separated components (Benkő, Szabó & Paparó 2011) and the irregularity of the modulation causes these components to be broadened. In Section 7.3, we will present arguments in favour of this latter interpretation.

The separation between the components of the f_2 multiplet can be used to estimate the time-scale of variability of this mode. For KIC 8832417 and KIC 4064484 we find ∼75 d and ∼29 d, respectively. In KIC 9453114 the separation implies time-scale of ∼19 d. However, in this object every second multiplet component is very weak. Therefore, variations of f_2 will be dominated by a time-scale half as long, i.e. ∼9.5 d. The derived numbers confirm our earlier assessment that the variability of the secondary mode is faster in stars of longer periods.

In the right-hand column of Fig. 8, we display the FT of the subharmonic, $3/2f_2$. This signal is visible only in the FT of the first three stars. In KIC 5520878 the peak is broadened, but not yet resolved into separate components. This is the same behaviour as displayed by its parent mode (f_2). In KIC 8832417 the subharmonic is already split, but because components are much broader than in the case of f_2, the splitting appears incomplete. Finally, in KIC 4064484 the subharmonic is resolved into three separate bands of power. In both KIC 8832417 and KIC 4064484, the splitting pattern of the subharmonic looks different than for its parent mode. Nevertheless, the *frequency separations* of multiplet components for $3/2f_2$ and for f_2 are roughly the same. This shows that both signals vary on approximately the same time-scale.

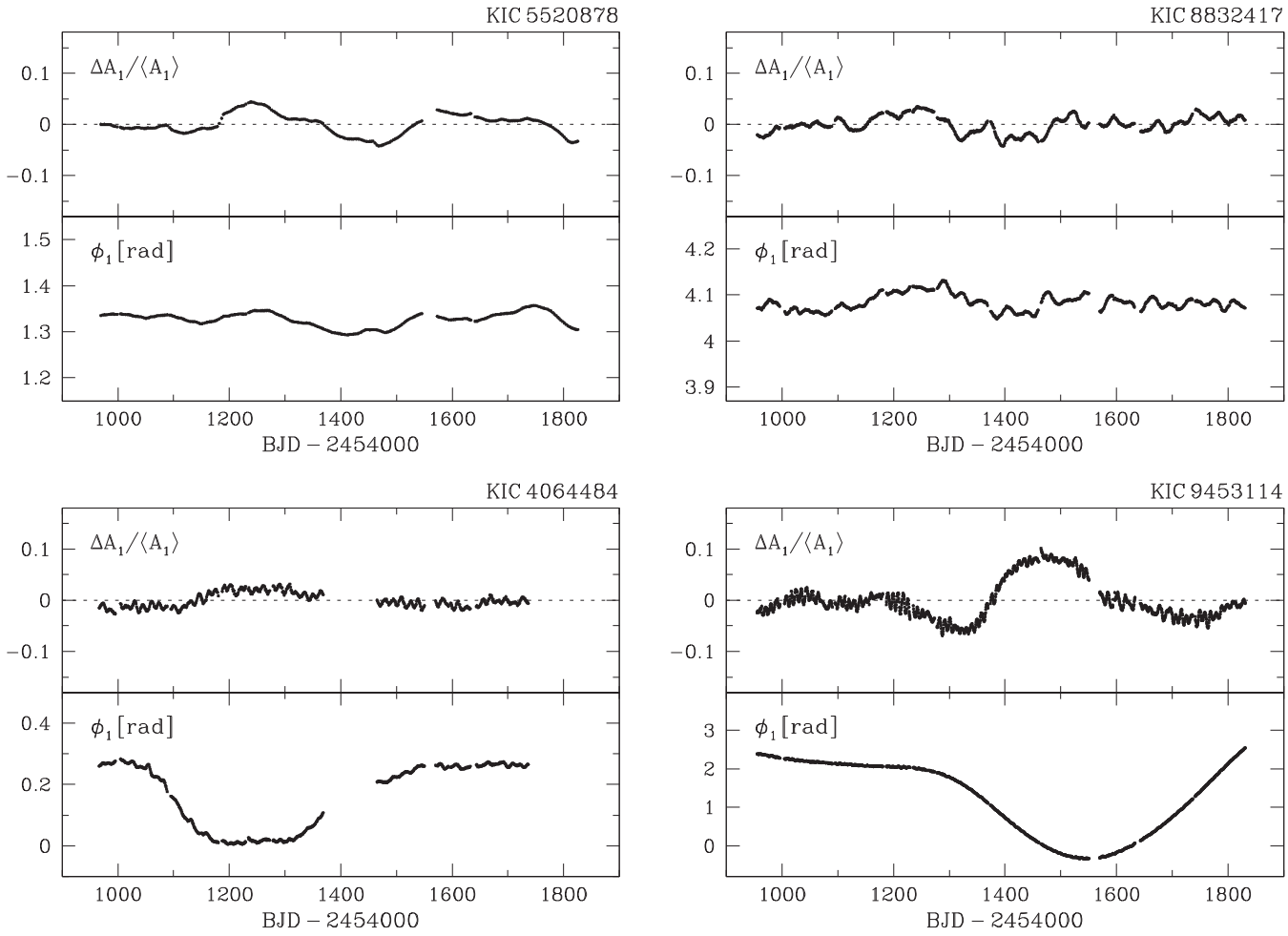

Figure 9. Amplitude and phase variations of the dominant radial mode in *Kepler* RRc stars.

5.2 The radial mode

5.2.1 Time domain

In Fig. 9, we show the temporal behaviour of the dominant radial mode in *Kepler* RRc stars. In every object, we find changes of both the amplitude (A_1) and the phase (ϕ_1). This variability has two components: a long-term drift with a time-scale of many months, and a much faster quasi-periodic modulation which is superimposed on this drift.

With the exception of KIC 9453114, the long-term amplitude changes are rather small, less than ±4 per cent. We are not sure if these changes are real. They might be of instrumental origin, resulting, e.g. from a slow image motion, coupled with a contamination by a nearby faint star. Amplitude fluctuations of this size are found in many stars observed with the *Kepler* telescope. On the other hand, the amplitude variations found in KIC 9453114 are much larger (±8 per cent) and they are almost certainly intrinsic to the star. We note that these variations do not resemble the Blazhko modulation as we currently know it (Benkő et al. 2010, 2014).

In two of the studied stars the radial mode displays a large, long-term drift of the pulsation phase, amounting to almost 0.3 rad in KIC 4064484 and 2.9 rad in KIC 9453114. These variations are orders of magnitude too fast to be explained by stellar evolution. We note that non-evolutionary phase changes are observed in many RRc and RRab stars (e.g. Jurcsik et al. 2001, Jurcsik et al. 2012, Le Borgne et al. 2007), as well as in many overtone Cepheids (e.g. Berdnikov et al. 1997; Moskalik & Kołaczkowski 2009). They are also occasionally detected in δ Sct stars (e.g. Bowman & Kurtz 2014). Currently, their nature remains unexplained (see however Derekas et al. 2004).

We now turn our attention to the short time-scale variations. They are clearly visible in three of the *Kepler* RRc stars: KIC 8832417, KIC 4064484 and KIC 9453114. These variations are very small: changes of A_1 are of the order of ±1.5 per cent, or equivalently of ±2.5 mmag, and changes of ϕ_1 of the order of ±0.01 rad. Such a small effect could be detected only with ultraprecise photometry, such as delivered by *Kepler*. The rapid variability of the radial mode is faster in stars of longer periods. We recall that the same tendency was found previously for the secondary mode, f_2. In Fig. 10, we compare temporal behaviour of the two modes in KIC 9453114. It is immediately obvious that the amplitude of the radial mode, A_1, and the amplitude of the secondary mode, A_2, vary with the same time-scale. We also note that the two amplitudes seem to be anticorrelated and a maximum (minimum) of one of them in most cases coincides with a minimum (maximum) of the other. This behaviour is common to all *Kepler* RRc stars.

Period variations. Phase variations of the dominant radial mode (Fig. 9) are equivalent to variations of its period, P_1. The latter can be computed with equation (2). Slow long-term phase drifts observed in KIC 4064484 and KIC 9453114 correspond to slow long-term

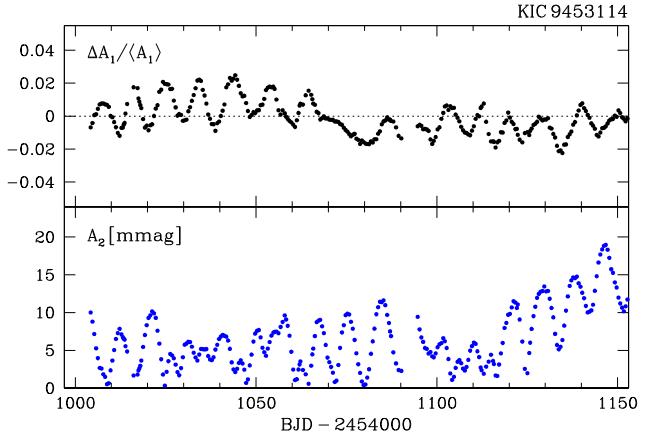

Figure 10. Amplitude variations in KIC 9453114. Upper panel: dominant radial mode, f_1. Bottom panel: secondary mode, f_2.

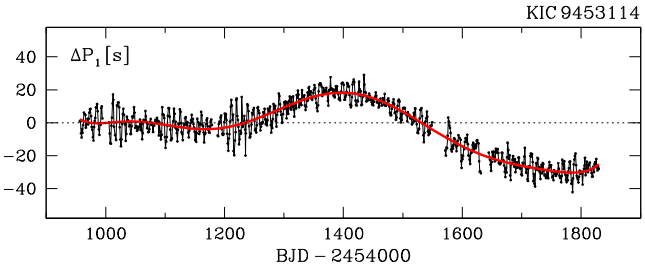

Figure 11. Period variations of the dominant radial mode in KIC 9453114. Fifth-order polynomial fit (red thick line) represents the slow period drift.

changes of P_1, with a total range of ∼7 s and ∼49 s, respectively. The short time-scale phase variations result in additional quasi-periodic modulation of P_1, imposed on the long-term trends. The maximum range of these rapid variations is ±3.2 s in KIC 8832417, ±5.0 s in KIC 4064484 and ±16.5 s in KIC 9453114. Changes of the radial mode period in the last object are displayed in Fig. 11.

5.2.2 *Frequency domain*

Because of quasi-periodic modulation, we expect the dominant radial mode to appear in the FT as a multiplet structured around the frequency f_1. Since the variations are very small (∼1.5 per cent in amplitude), the modulation sidepeaks should be *much lower* than the central peak of the multiplet. Therefore, in order to extract them from the FT, we first need to remove the central peak.

This is not a straightforward task. The amplitude A_1 and phase ϕ_1 of the radial mode undergo slow long-term changes (Fig. 9). As a result, the central component of the multiplet is not coherent. The standard pre-whitening method will fail in such a case, leaving unremoved residual power. To remedy this situation, we applied the *time-dependent pre-whitening*, a new technique described in Appendix A. In this procedure, we subtract from the light curve a sine wave with varying amplitude and phase. The functional form of $A_1(t)$ and $\phi_1(t)$ is determined by the time-dependent Fourier analysis of the data. With the proper choice of the length of the light curve segment, Δt, we can remove the central peak of the multiplet, leaving the sidepeaks unaffected. The appropriate value of Δt has to be longer than the quasi-period of the modulation, but short enough to capture the long-term drift of A_1 and ϕ_1.

Table 5. Low-amplitude periodicities in KIC 5520878.

Frequency	f (d^{-1})	A (mmag)
f_4	1.032 72	0.11
f_{5a}	1.125 35	0.35
f_{5b}	1.135 77	0.33
$f_{5a} - f_1$	2.590 12	0.07
$f_{5b} - f_1$	2.5793	0.04
$f_{5a} - 2f_1$	6.3049	0.04
$f_{5b} - 2f_1$	6.2941	0.03
$f_{5a} - 3f_1$	10.0201	0.04
$f_{5b} - 3f_1$	10.0094	0.03
$f_{5a} - 4f_1$	13.7353	0.03
$f_{5b} - 4f_1$	13.7245	0.03
$f_{5a} + f_1$	4.840 70	0.20
$f_{5b} + f_1$	4.850 87	0.21
$f_{5a} + 2f_1$	8.5558	0.04
$f_{5b} + 2f_1$	8.566 11	0.06
$f_{5a} + 3f_1$	12.2709	0.03
$f_{5b} + 3f_1$	12.2813	0.03
$f_{5a} + 4f_1$	15.9859	0.03
f_{6a}	1.498 77	0.14
f_{6b}	1.503 17	0.19
f_{6c}	1.506 86	0.11
$f_{6b} + f_1$	5.218 14	0.13
$f_{6b} + 2f_1$	8.9332	0.05
$f_{6b} + 3f_1$	12.6483	0.03
f_7	1.800 60	0.06
f_8	2.638 91	0.08
f_9	2.759 26	0.10
$f_9 + f_1$	6.4744	0.04
f_{10a}	2.776 51	0.19
f_{10b}	2.779 00	0.19
f_{10c}	2.781 41	0.22
$f_{10a} + f_1$	6.491 65	0.08
$f_{10b} + f_1$	6.494 19	0.08
$f_{10c} + f_1$	6.496 45	0.08
$f_{10a} + 2f_1$	10.2067	0.03
f_{11}	4.699 68	0.18
$f_{11} - f_1$	0.980 52	0.14
$f_{11} - 2f_1$	2.728 74	0.06
$f_{11} + f_1$	8.414 79	0.05
$f_{11} + 2f_1$	12.1298	0.04
f_{12a}	10.721 26	0.09
f_{12b}	10.72867	0.07
$f_{12a} - f_1$	7.0061	0.05
$f_{12a} + f_1$	14.4363	0.04
$f_{12a} + 2f_1$	18.1516	0.03
$f_{12b} + 2f_1$	18.1586	0.02

We applied this technique to all *Kepler* RRc stars except KIC 5520878, for which the radial mode does not show any short time-scale variations. In Fig. 12 (bottom panels), we display the pre-whitened FT of the radial mode in KIC 8832417, KIC 4064484 and KIC 9453114. For removing the central peak of the multiplet we adopted $\Delta t = 100$, 30 and 20 d, respectively. In the upper panels of the figure, we plot for comparison the frequency pattern of the secondary mode, f_2. In each of the three stars, the dominant radial mode, f_1, splits into a quintuplet of equally spaced peaks. This is particularly well visible for KIC 4064484, where the structure is nicely resolved and very clean. In KIC 9453114 the quintuplet pattern is also clear, but additional peaks appearing in the vicinity of $\Delta f = -0.10$ d^{-1} and $\Delta f = +0.07$ d^{-1} slightly confuse the picture. Compared to f_2, the modulation side peaks of the radial mode

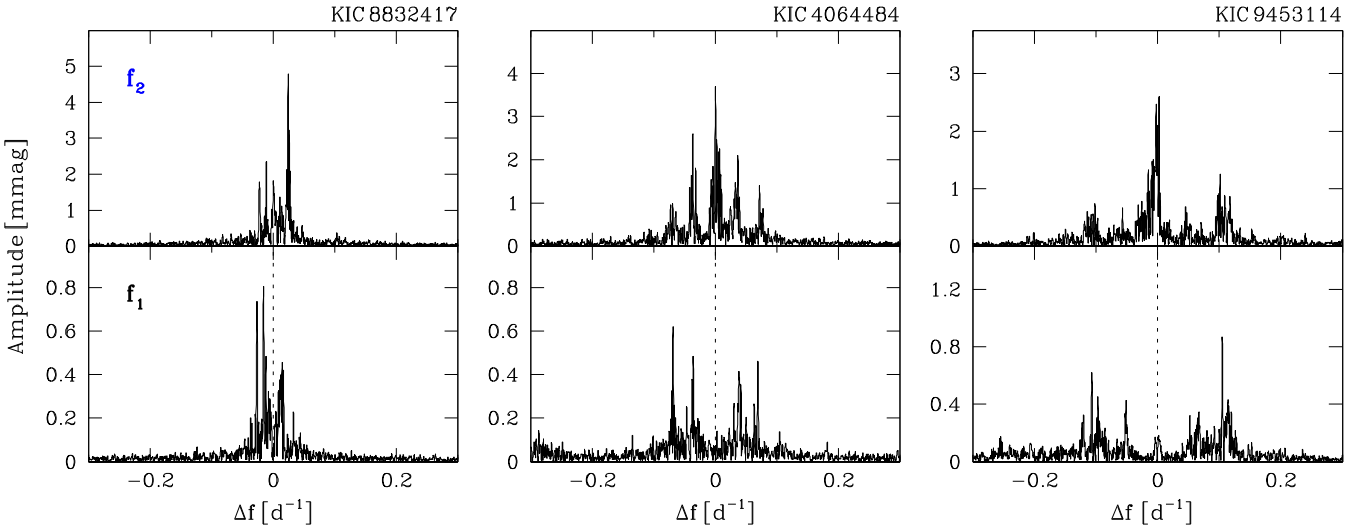

Figure 12. Frequency splitting for primary and secondary modes of *Kepler* RRc stars (for entire Q0 − Q10 light curves). Upper panels: FT of the secondary mode, f_2. Bottom panels: FT of the dominant radial mode, f_1. The central component of the f_1 multiplet (indicated by the dashed line) has been subtracted.

are significantly narrower (i.e. more coherent). They are also much lower, never exceeding 0.9 mmag. This latter property bears witness to the extremely low amplitude of the radial mode modulation. Apart from these differences, the quintuplet splitting patterns of f_1 and f_2 are very similar. In particular, while separation between the quintuplet components differs from star to star, it is always *the same for both modes*. This means that the secondary mode, f_2, and the dominant radial mode, f_1, are both modulated with a common time-scale.

6 ADDITIONAL FREQUENCIES

A FT of the entire light curve (Q0 − Q10) offers not only better frequency resolution, but also a much lower noise level than the FT computed from a single quarter of data (Figs 4 and 5). This advantage can be used to search for additional, low amplitude periodicities hidden in the light curve.

6.1 KIC 5520878

In order to lower the noise in the FT as much as possible, we first subtracted from the light curve the dominant frequency f_1 and its harmonics, as well as eight other frequency components higher than 0.4 mmag ($f_2, f_2 - f_1, f_1 + f_2, 2f_1 + f_2, 1/2f_2, 3/2f_2, f_1 - 1/2f_2$, $f_1 + 3/2f_2$). This step was performed with the time-dependent pre-whitening method, adopting $\Delta t = 20$ d. The pre-whitened FT yields a rich harvest of additional low-amplitude periodicities. We list them in Table 5. Four segments of the pre-whitened FT are displayed in Fig. 13.

In total, we detected 46 new, significant frequencies. All have amplitudes below 0.4 mmag. We checked that none of them can be explained as a linear combination of f_1, f_2 or $1/2f_2$. Only 15 of the new frequencies are independent, i.e. correspond to pulsation modes. The remaining frequencies are linear combinations of the independent ones and f_1. In fact, except of f_4, f_7 and f_8, all other independent frequencies generate at least one combination peak. This is a very important observation. It proves that these periodicities originate in KIC 5520878 itself, and are not introduced by blending with another star.

The strongest of the low-amplitude modes appear at $f_{5a} = 1.125\,35$ d^{-1} and $f_{5b} = 1.135\,77$ d^{-1}. These two modes form a well-resolved doublet. The same doublet structure is apparent in their linear combinations with f_1. Another well-resolved doublet with slightly smaller separation is formed by $f_{12a} = 10.721\,26$ d^{-1} and $f_{12b} = 10.728\,67$ d^{-1}. Two equidistant triplets are also found: f_6 with separation of $\delta f_6 = 0.004\,05$ d^{-1} and f_{10} with separation of $\delta f_{10} = 0.002\,45$ d^{-1}. With the timebase of 869 d, we consider the f_{10} triplet to be only marginally resolved. We note that δf_{10} is not very different from $1/372.5$ d $= 0.002\,68$ d^{-1}. Therefore, splitting of f_{10} might be an artefact, caused by the instrumental amplitude variation with the orbital period of the telescope. We think this is unlikely. If such a modulation is present in the data, it should affect *all* the frequencies. Clearly, this is not the case. Judging from behaviour of the dominant radial mode (Fig. 9), any instrumental amplitude variation in the KIC 5520878 data set cannot be larger than ±4 per cent. Such a small modulation cannot explain relatively large sidepeaks of the f_{10} triplet.

Two modes attract special attention. For f_9 and f_{10}, we find period ratios of $P_1/P_9 = 0.7427$ and $P_1/P_{10} = 0.7480$, respectively. These values are close to canonical period ratio of the radial first overtone and radial fundamental mode in the RR Lyrae stars (Kovács 2001; Moskalik 2014). This suggests that either f_9 or f_{10} might correspond to the radial fundamental mode. However, such a conclusion would be too hasty. In the case of the RR Lyrae stars, there is an empirical relation between the period ratio of the two lowest radial modes, P_{1O}/P_F and the pulsation period itself. P_{1O}/P_F is a steep function of P_F and at short periods it becomes considerably lower than 0.74. This is best demonstrated by the double-mode RR Lyrae pulsators (RRd stars) of the Galactic Bulge (Soszyński et al. 2011a). When plotted on the Petersen diagram, i.e. period ratio versus period diagram (their fig. 4), the Bulge RRd stars form a narrow, well-defined sequence, which extends down to $P_{1O}/P_F \sim 0.726$ at a fundamental-mode period of $P_F \sim 0.347$ d. It is easy to check that neither P_1/P_9 nor P_1/P_{10} conforms to this empirical progression. Using fig. 4 of Soszyński et al. (2011a), we can estimate that the radial fundamental mode in KIC 5520878 should have a period of $P_F = 0.3677$–0.3692 d ($f_F = 2.7084$–2.7194 d^{-1}), corresponding to a period ratio of $P_{1O}/P_F \equiv P_1/P_F = 0.729$–$0.732$. We conclude, therefore, that none of the

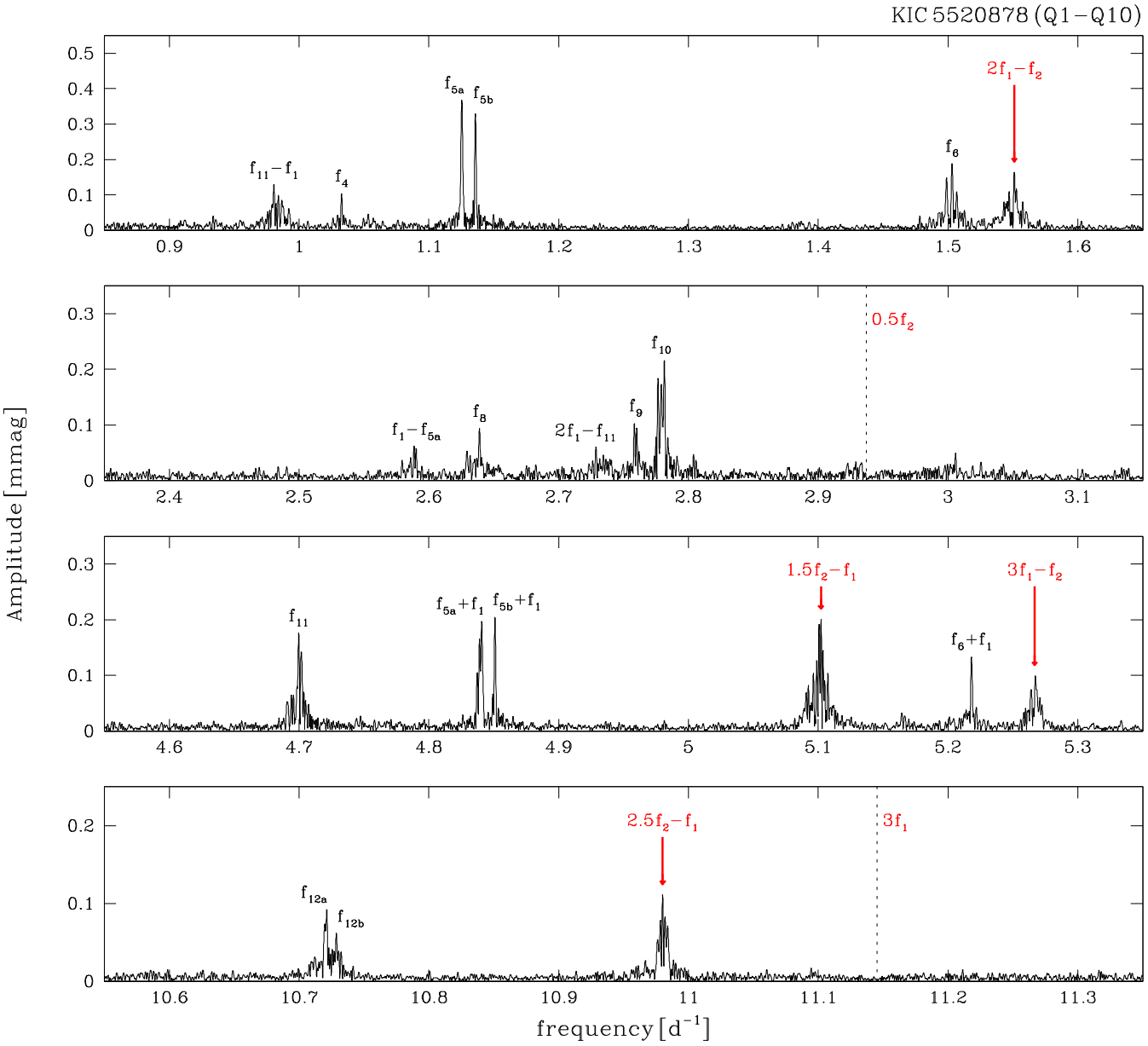

Figure 13. Additional low-amplitude frequencies in KIC 5520878. Frequency spectrum was computed for the entire light curve (Q1 – Q10), pre-whitend of the dominant radial mode, its harmonics and all peaks higher than 0.4 mmag. Dashed lines indicate subtracted frequencies $1/2f_2$ and $3f_1$.

frequencies detected in KIC 5520878 can be identified with the radial fundamental mode.

Another frequency of special interest is f_{11}. In the case of this mode, we find a period ratio of $P_{11}/P_1 \equiv P_{11}/P_{1O} = 0.7905$. This value is close to period ratios measured in double overtone Cepheids, particularly in those of the Galactic Bulge and the Galactic field (Soszyński et al. 2008, 2010, 2011b; Smolec & Moskalik 2010 and references therein). We do not know 1O+2O pulsators among the RR Lyrae stars, so we cannot compare their period ratios with P_{11}/P_1. But we can proceed differently – using the estimated period of the radial fundamental mode in KIC 5520878, we can estimate $P_{11}/P_F = 0.576$–0.579. This value is very close to the empirical period ratio of the F+2O double-mode RR Lyrae pulsators (Moskalik 2013). On this basis, we identify f_{11} with the radial second overtone.

Except for f_{11}, all the remaining low-amplitude modes detected in KIC 5520878 must be nonradial. We note that most of them (f_4, f_5, f_6, f_7, f_8) have frequencies lower than the (unobserved) radial fundamental mode. This implies that these are not p-mode oscillations, they must be classified as gravity modes (g-modes). This is the first detection of such modes in RR Lyrae stars.

6.2 KIC 4064484, KIC 8832417 and KIC 9453114

In the other three *Kepler* RRc stars only very few additional low-amplitude modes can be found. In KIC 8832417 and KIC 9453114, we detected five and two such modes, respectively. Their frequencies are listed in Tables 6 and 7. About half of them generate linear combinations with the dominant frequency, f_1. None of the low-amplitude modes can be identified with the radial fundamental or

Table 6. Low-amplitude periodicities in KIC 8832417.

Frequency	f (d^{-1})	A (mmag)
f_4	1.186 53	0.25
$f_4 + f_1$	5.209 90	0.12
f_{5a}	3.085 89	0.07
f_{5b}	3.093 47	0.08
f_6	6.656 58	0.32
$f_6 - f_1$	2.633 15	0.10
$f_6 + f_1$	10.679 88	0.11
f_7	9.515 94	0.08

Table 7. Low-amplitude periodicities in KIC 9453114.

Frequency	f (d^{-1})	A (mmag)
f_4	0.911 99	0.23
$f_4 + f_1$	3.643 15	0.10
f_5	1.875 88	0.92
$f_5 - f_1$	0.856 17	0.10
$f_5 - 2f_1$	3.587 50	0.16

with the second radial overtone. As in KIC 5520878, some of the modes have frequencies lower than the fundamental radial mode. Therefore, they must be g-mode type. This is the case for f_4 in KIC 8832417 and for both f_4 and f_5 in KIC 9453114.

The strongest of the low-amplitude modes detected in KIC 8832417 is of particular interest. Its frequency $f_6 = 6.656\,58$ d^{-1} yields a period ratio of $P_6/P_1 = 0.6044$, which is very close to $P_2/P_1 = 0.6122$. Apparently, in this star there are two modes with period ratios in the range of 0.60–0.63.

No frequencies beyond $f_1, f_2, 3/2f_2$ and their combinations were found in KIC 4064484.

7 DISCUSSION

7.1 A new period ratio for RR Lyrae stars

It is striking that all four RRc stars prominent in the *Kepler* field that have been analysed in this paper show an additional frequency with a period ratio of ∼0.61 to the main radial mode. This is not the first time such a period ratio has been seen in RR Lyrae stars. It was first found in a double-mode variable AQ Leo (Gruberbauer et al. 2007). Since then, low-amplitude modes yielding similar period ratios have been detected in 18 other RR Lyrae variables, observed both from the ground and from space. We list these objects in Table 8, where we also include, for completeness, the four *Kepler* RRc stars. For each variable we provide its pulsation type, a period of the dominant radial mode, P_1, a period ratio of the secondary mode and the dominant mode, P_2/P_1, and an amplitude of the secondary mode, A_2. In the case of double-mode variables in which two radial modes are present, P_1 refers to the *first radial overtone*. The amplitudes A_2 are given in different photometric systems by different authors and, consequently, are not directly comparable to each other. We quote them here only to provide a rough estimate of the strength of the secondary mode.

Comments on individual stars

ω Cen variables V10, V81, V87 and V350. Detection of the secondary mode in these stars is unambiguous, but identification of its true period is hindered by daily aliases. Depending on the choice of an alias we find period ratio of either $P_2/P_1 \sim 0.80$ or ∼0.61. Only in the case of V10 is the former alias slightly higher, which led Olech & Moskalik (2009) to designate this variable a candidate double overtone pulsator. In V81, V87 and V350 the latter alias is higher. So far, no unambiguous 1O+2O double-mode RR Lyrae stars have been found in any stellar system (see, however, Pigulski

Table 8. Known RR Lyrae variables with $P_2/P_1 \sim 0.61$.

Star	Type	P_1 (d)	P_2/P_1	A_2 (mmag)	Subharmonics of f_2	Ref.
ω Cen V10	RRc	0.3750	0.6137	6.4		2
ω Cen V19	RRc	0.3000	0.6119	7.1		2
ω Cen V81	RRc	0.3894	0.6138	7.2		2
ω Cen V87	RRc	0.3965	0.6219	6.3		2
ω Cen V105	RRc	0.3353	0.6138	12.5		2
ω Cen V350	RRc	0.3791	0.6084	6.2		2
OGLE-LMC-RRLYR-11983	RRc	0.3402	0.6026	51.5:		3
OGLE-LMC-RRLYR-14178	RRc	0.3634	0.6103	27.8:		3
SDSS Stripe 82-1528004	RRc:	0.3276	0.6068	?		4
SDSS Stripe 82-3252839	RRc	0.3112	0.6238	?		4
CoRoT 0105036241	RRc	0.3729	0.6125	3.3		6
CoRoT 0105735652	RRc	0.2792	0.6150	2.2		6
KIC 4064484	RRc	0.3370	0.6156	4.6	yes	7
KIC 5520878	RRc	0.2692	0.6320	7.0	yes	7
KIC 8832417	RRc	0.2485	0.6122	7.1	yes	7
KIC 9453114	RRc	0.3661	0.6144	4.6	yes	7
EPIC 60018224	RRc	0.3063	0.6145	11.4	yes	8
EPIC 60018238	RRc	0.2748	0.6030	2.0		8
EPIC 60018678	RRc	0.4325	0.6200	3.8	(yes)	8
AQ Leo	RRd	0.4101	0.6211	2.5	yes	1
CoRoT 0101368812	RRd	0.3636	0.6141	5.5	yes	5
EPIC 60018653	RRd	0.4023	0.6163	8.5	yes	8
EPIC 60018662	RRd	0.4175	0.6170	6.9	yes	8

REFERENCES: 1 – Gruberbauer et al. (2007); 2 – Olech & Moskalik (2009); 3 – Soszyński et al. (2009); 4 – Süveges et al. (2012); 5 – Chadid (2012); 6 – Szabó et al. (2014); 7 – this paper; 8 – Molnár et al., in preparation.

2014). On the other hand, the existence of RR Lyrae stars with $P_2/P_1 \sim 0.61$ is well established. On these grounds, we consider the period ratio of ∼0.61 to be more likely in these four variables.

ω Cen variables V19 and V105. In these stars the identification of the correct alias and consequently of the true period of the secondary mode is unambiguous.

OGLE-LMC-RRLYR-11983. In the original paper of Soszyński et al. (2009), the star was classified as a fundamental mode pulsator (RRab star). This was based on the measured value of the Fourier phase ϕ_{21}. However, the harmonic of the primary mode in this variable is weak and its amplitude is determined with a large error of almost 30 per cent. Consequently, ϕ_{21} is not measured accurately enough to distinguish between an RRc and an RRab light curve. In fact, $\phi_{21} = 3.358$, derived by Soszyński et al. (2009), does not fit to either type. We have reclassified this star using the empirical period luminosity relation for the Wesenheit index, $W_I = I - 1.55(V - I)$. With $W_I = 18.376$ mag, OGLE-LMC-RRLYR-11983 is placed firmly among the RRc stars of the Large Magellanic Cloud (LMC).

OGLE-LMC-RRLYR-14178. The star was classified by Soszyński et al. (2009) as an overtone pulsator (RRc star). The value of the Wesenheit index $W_I = 17.795$ mag supports this classification.

SDSS Stripe 82 variables 1528004 and 3252839. The secondary frequency in these stars was detected with a principal component analysis, applied to multiband photometric data (Süveges et al. 2012). The authors did not identify the dominant radial mode. On the basis of the empirical period-amplitude diagram (their fig. 9) we classify variable 3252839 as an RRc star. In the case of 1528004, the period of the radial mode points towards overtone pulsations, but its amplitude is too high for an RRc type. We classify this variable as a probable RRc star. Amplitudes of the secondary mode were not published.

CoRoT 0105036241 and CoRoT 0105735652. The secondary mode in these stars was detected with photometry collected by the *CoRoT* space telescope (Szabó et al. 2014). No subharmonics were found.

EPIC 60018224 ≡ *EV Psc*. The secondary mode was discovered during 9-d long engineering test run of *Kepler* K2 mission (Molnár et al., in preparation). Subharmonics of the secondary mode at $\sim 1/2f_2$ and $\sim 3/2f_2$ are also clearly visible.

EPIC 60018238. No subharmonics of the secondary mode were detected in this star.

EPIC 60018678. In addition to the secondary mode, marginally significant subharmonics at $\sim 1/2f_2$ and $\sim 3/2f_2$ are also present in this star (Molnár et al., in preparation).

AQ Leo. The secondary mode in this double-mode star was discovered with photometry collected by the *MOST* space telescope (Gruberbauer et al. 2007). A subharmonic of a secondary mode at $\sim 1/2f_2$ was also found, although it was not recognized as such at the time.

CoRoT 0101368812. The secondary mode with a period ratio of ∼0.61 to the first radial overtone was discovered by Chadid (2012). In addition, its subharmonic at $\sim 3/2f_2$ was also detected, but not recognized as such by the author. It is denoted in the original paper as $f_4 - f_1$.

EPIC 60018653. In addition to the secondary mode, subharmonics at $\sim 1/2f_2$ and $\sim 3/2f_2$ are also clearly visible in this star (Molnár et al., in preparation).

EPIC 60018662. In addition to the secondary mode, a weak subharmonic at $\sim 1/2f_2$ was also detected in this star (Molnár et al., in preparation).

Objects listed in Table 8 form a sample of 23 RR Lyrae variables in which a period ratio of ∼0.61 has been found. In most of these stars the main mode is the first radial overtone (RRc type). Four variables belong to the group of double-mode pulsators (RRd type), where two radial modes are excited. Even in the latter case, the first radial overtone strongly dominates, having an amplitude 1.8–3.0 times higher than the fundamental mode (Gruberbauer et al. 2007; Chadid 2012; Molnár et al., in preparation). In Fig. 14, we plot all 23 stars on the Petersen diagram. They form a tight, almost horizontal progression, with values of P_2/P_1 restricted to a narrow range of 0.602–0.632. Both RRc and RRd variables follow the same trend. Clearly, the RR Lyrae star with $P_2/P_1 \sim 0.61$ form a highly homogenous group, constituting a *new, well-defined class of multimode pulsators*.

In all stars of this class the amplitude of the additional mode is extremely low, in the mmag range. This amplitude is typically 20–60 times lower than the amplitude of the dominant radial mode. Detection of such a weak signal from the ground is difficult. The situation is very different for stars observed from space. With the sole exception of the Blazhko star CSS J235742.1–015022 (Molnár et al., in preparation), the secondary mode yielding period ratio of $P_2/P_1 \sim 0.61$ has been detected in *every* RRc and RRd pulsator for which high-precision space photometry is available. This is 13 objects out of total 14 observed from space. Such statistics strongly suggest that excitation of this additional mode is not an exception. It must be a common property of RRc and RRd variables. We expect that it should be found in many more stars, provided that good enough data become available.

7.1.1 Comparison with Cepheids

Detection of low amplitude secondary modes with a period ratio of ∼0.61 to the main radial mode is not limited to the RR Lyrae stars. Similar modes are also found in Classical Cepheids of the Magellanic Clouds. So far, 173 such variables have been identified (Moskalik & Kołaczkowski 2008, 2009; Soszyński et al. 2008, 2010). In Fig. 15, we plot them on the Petersen diagram, together with their RR Lyrae counterparts. Both groups have very similar properties. In the case of Cepheids, just like in the RR Lyrae stars, the phenomenon occurs only in the first overtone variables or in the double-mode variables pulsating simultaneously in the fundamental mode and the first overtone (only one star). Apparently, excitation of the first radial overtone is a necessary condition. The amplitudes of the secondary modes are as low as in the RR Lyrae stars, with amplitude ratios of $A_2/A_1 < 0.055$ (Moskalik & Kołaczkowski 2009). The measured period ratios are also almost the same in both types of pulsators, although in Cepheids the range of P_2/P_1 is somewhat broader (0.599–0.647). The only difference between the two groups is that Cepheids split in the Petersen diagram into three well-detached parallel sequences, whereas no such structure is evident in the case of RR Lyrae stars. This difference needs to be explained by future theoretical work.

7.1.2 Comparison with theoretical calculations

In the case of Classical Cepheids it has been shown that the period ratio of ∼0.61 cannot be reproduced by two radial modes (Dziembowski & Smolec 2009; Dziembowski 2012). Since the main mode is radial, this implies that the secondary frequency, f_2, must correspond to a non-radial mode of oscillation. Theoretical analysis

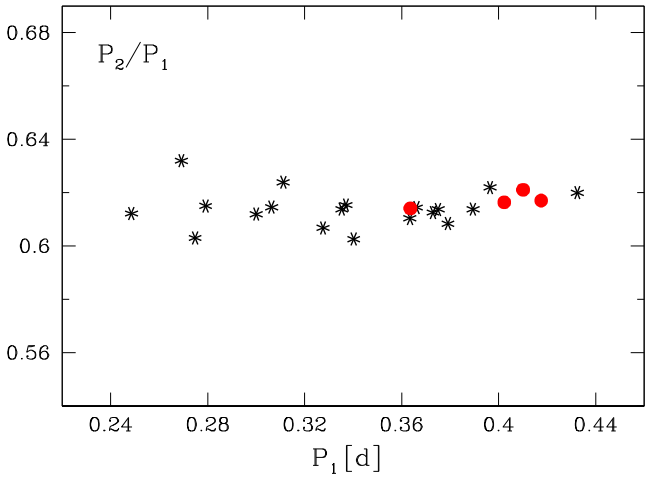

Figure 14. Petersen diagram for RR Lyrae stars of Table 8. RRc stars are plotted with black asterisks and RRd stars with red filled circles.

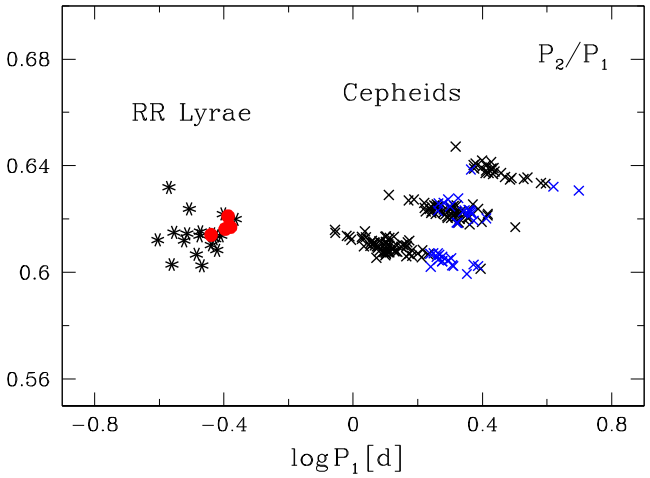

Figure 15. Petersen diagram for RR Lyrae stars and Cepheids with period ratios of 0.60–0.65. For the RR Lyrae variables, the same symbols as in Fig. 14 are used. Cepheids of SMC and LMC are plotted with black and with blue crosses, respectively.

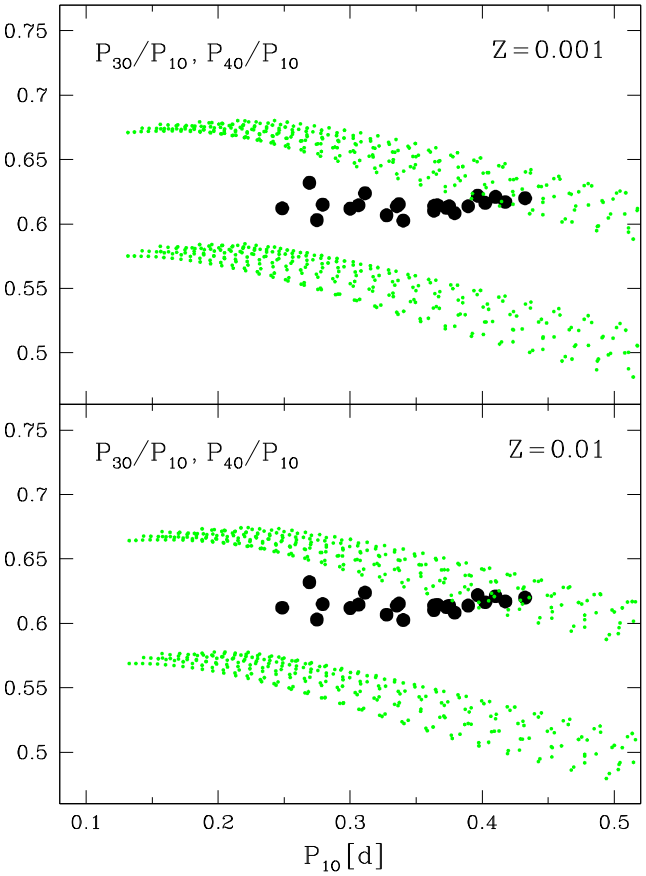

Figure 16. Linear period ratios P_{3O}/P_{1O} and P_{4O}/P_{1O}. Model masses and luminosities are in the range of 0.55–0.75 $M_{\odot}$ and 40–70 $L_{\odot}$, respectively. Upper panel: models for metallicity of $Z = 0.001$. Bottom panel: models for metallicity of $Z = 0.01$. The RR Lyrae stars of Table 8 are plotted with filled circles for comparison.

indicates that an f-mode of high spherical degree ($\ell = 42$–50) is the most likely candidate (Dziembowski 2012).

The same argument for non-radial nature of f_2 can also be made for RR Lyrae stars. In Fig. 16, we present theoretical Petersen diagrams for two different metallicities, $Z = 0.001$ and 0.01. Period ratios of the third-to-first (P_{3O}/P_{1O}) and fourth-to-first (P_{4O}/P_{1O}) radial overtones have been computed with the Warsaw linear pulsation code (Smolec & Moskalik 2008a). Our calculations cover a range of masses, luminosities and effective temperatures spanning the entire domain of the RR Lyrae stars. For metallicity $Z = 0.01$, the theoretical period ratios are systematically lower than for $Z = 0.001$, but the difference is not large. Further increase of Z does not lower the computed values any further. We note in passing, that weak sensitivity to Z is typical of period ratios of two overtones. This is different from behaviour of P_{1O}/P_F, sensitivity of which to a metal abundance is much stronger (see e.g. Popielski et al. 2000). The models are compared with the RRc and RRd variables listed in Table 8. The observed period ratios generally fall between theoretically predicted values of P_{3O}/P_{1O} and P_{4O}/P_{1O}. Only in a handful of long period variables can the secondary period be matched with the third overtone, but for vast majority of the sample it cannot be matched with a radial mode. This result does not depend on the choice of Z. Therefore, as in the case of Cepheids, we conclude that also in the RR Lyrae stars the secondary mode with a period ratio of ∼0.61 to the first radial overtone must be non-radial.

Model calculations show that two different types of non-radial modes are linearly unstable in the RR Lyrae stars (Van Hoolst, Dziembowski & Kawaler 1998; Dziembowski & Cassisi 1999). Low-degree modes of $\ell = 1$–3 are excited rather weakly and preferentially in the vicinity of radial modes. Their frequency spectrum is very dense, which makes it difficult to destabilize only a single isolated mode. The other group are strongly trapped unstable modes (STU modes) of high spherical degree ($\ell \geq 6$). Oscillations of this type are excited strongly, with growth rates as large as in the case of radial modes. Most importantly, such oscillations can be excited at frequencies far apart from those of the radial modes. The strong trapping in the envelope, which makes their destabilization possible, usually selects from the dense spectrum only a single mode. We believe that excitation of STU modes is the most likely explanation for the puzzling period ratio of ∼0.61 in the RRc and RRd variables. At this point, this is only a working hypothesis. Its verification requires detailed linear non-adiabatic pulsation calculations, similar to those performed by Dziembowski (2012) for the Classical Cepheids.

7.2 Period doubling of the secondary mode

In all four *Kepler* RRc stars not only do we see the additional frequency with a period ratio of ∼0.61 to the main mode, but we also see its subharmonics at $\sim 1/2f_2$ and $\sim 3/2f_2$. Subharmonic frequencies are also detected in several other variables of Table 8. Noticeably, they are found only in those stars for which high-precision space photometry is available. This is hardly surprising, considering that amplitudes of the subharmonics are even lower than in the case of f_2, and almost never exceed 3.0 mmag. In total, the additional mode f_2 is accompanied by subharmonics in 10 out of 13 RRc and RRd stars studied from space. Clearly, this is a common property of these variables.

The presence of subharmonics in the frequency spectra of RRc and RRd stars is very significant, as it is a characteristic signature of a period doubling behaviour. Period doubling is a phenomenon which is well known in many dynamical systems (Bergé et al. 1986). In the context of stellar pulsations, it results in an alternating light curve in which even and odd pulsation cycles have different shapes. Such a light curve repeats itself after *two* pulsation periods, not one. The appearance of subharmonics in the Fourier spectrum is a direct consequence of this property (e.g. Smolec & Moskalik 2012, their fig. 3).

Light curves with alternating deep and shallow minima have been known for decades in RV Tauri stars. Only in the 1980s were they interpreted as resulting from period doubling (Buchler & Kovács 1987; Kovács & Buchler 1988). More recently, the period doubling effect has been discovered in two other types of pulsating variables – in Blazhko-modulated RRab stars (Kolenberg et al. 2010; Szabó et al. 2010) and in BL Herculis stars (Smolec et al. 2012). In the former case, its strength varies significantly over the Blazhko cycle, and does not repeat from one Blazhko cycle to the next. The picture is different in the BL Herculis stars, where the alternating light curve is strictly periodic (repetitive).

As was first recognized by Moskalik & Buchler (1990), period doubling in pulsating variables can be caused by a half-integer resonance between the modes. Through hydrodynamical modelling, its origin in RV Tauri stars was traced back to the 5:2 resonance with the second overtone (Moskalik & Buchler 1990), in RRab stars to the 9:2 resonance with the ninth overtone (Kolláth, Molnár & Szabó 2011) and in BL Herculis stars to the 3:2 resonance with the first overtone (Buchler & Moskalik 1992; Smolec et al. 2012). In these three classes of pulsators the period doubling affects the dominant mode. In the case of the *Kepler* RRc stars and the other RRc and RRd stars of Table 8, however, we do not observe this phenomenon in the main radial mode(s). Instead, it is the puzzling *secondary non-radial mode* with a period ratio of ∼0.61 to the first overtone, that shows a period doubling behaviour. Therefore, as we do not know the identity of this mode, it is unclear which resonance (if any) is responsible for the period doubling in the RRc and RRd variables.

7.3 Variability of the secondary mode

In all four RRc stars observed with *Kepler*, the secondary non-radial mode, f_2, and its subharmonics at $\sim 1/2f_2$ and $\sim 3/2f_2$ display very strong variations of amplitudes and phases. Variability of the f_2 mode has also been found in other RRc stars observed from space (Szabó et al. 2014; Molnár et al., in preparation), indicating that this is yet another common property of all RRc pulsators.

Thanks to the superb quality of the *Kepler* data, we have been able to study this phenomenon with unprecedented detail. We have shown that variability of the secondary mode is quasi-periodic and occurs on a time-scale of 10–200 d, depending on the star. In the frequency domain, it causes the mode to split into a quintuplet of equally spaced peaks. Each of these peaks is broadened, which reflects an irregular character of the modulation. The main radial mode, f_1, also varies in a quasi-periodic way, but this modulation is extremely small. In the frequency domain, the mode splits into a quintuplet as well. In every star the separation between the quintuplet components of f_1 and of f_2 is the same, which proves that both modes are variable with the same time-scale.

The finding that the secondary mode and the main radial mode are both modulated on a common time-scale has implications for understanding of the nature of the f_2 multiplet. Because f_1 corresponds to a radial mode ($\ell = 0$), its quintuplet structure cannot be caused by rotational splitting. It can be interpreted only in one way – as resulting from a true, physical modulation of the mode's amplitude and phase. The same frequency splitting and thus the same variability time-scale of f_1 and f_2 indicates that modulations of the two modes are not independent. This in turn implies that quintuplet pattern of f_2 cannot correspond to a multiplet of non-radial modes, either. Accepting such a picture would make it difficult to understand why beating of rotationally split multiplet (f_2) should occur on the same time-scale as the true modulation of another mode (f_1). We believe that such a coincidence is highly unlikely. This leads us to the conclusion that the observed modulation of the secondary mode, f_2, is due not to beating, but just as in the case of f_1, to a true physical modulation of a single pulsation mode.

The same modulation time-scale of f_1 and f_2 implies that both modes must be part of the same dynamical system, in other words that they must interact with each other. We can only speculate what the nature of this interaction might be. Cross-saturation is the most obvious possibility that comes to mind. In physical terms, the two modes compete for the same driving (κ-mechanism in the He^+ partial ionization zone) and when the amplitude of one mode decreases, the amplitude of the other mode can increase. This kind of coupling *has to occur* always when the two modes use the same driving source. It also predicts that the amplitude variations of the two modes should be anticorrelated. This is what we observe.

8 SUMMARY AND CONCLUSIONS

In this paper, we present an in-depth analysis of four first overtone RR Lyrae stars (RRc stars) observed with the *Kepler* space telescope: KIC 4064484, KIC 5520878, KIC 8832417 and KIC 9453114. For our study, we used the LC data (30 min sampling) gathered between Q0 and Q10, with a total timebase of 774–880 d, depending on the star. Our most important findings can be summarized as follows.

(i) None of the studied *Kepler* RRc stars displays a classical Blazhko effect, with a nearly coherent periodic (or multiperiodic) modulation of the amplitude and phase of the dominant radial mode.

(ii) In every *Kepler* RRc star we detect a secondary mode, f_2, with a period ratio of ∼0.61 to the first radial overtone. The mode has a very low amplitude, more than 20 times below that of the dominant radial mode.

(iii) Secondary modes with similar period ratios are also present in 19 other RR Lyrae variables. These stars are either of RRc or of RRd type, but never of RRab type. Apparently, the excitation of the secondary mode is somehow connected with the excitation of the first radial overtone. The observed period ratios are in a very narrow range of 0.602–0.632, defining a new class of multimode

pulsators. Including the four RRc stars studied in this paper, this class has currently 23 members.

(iv) The period ratio of ∼0.61 is also observed in Classical Cepheids of the Magellanic Clouds. The stars are either single mode first overtone pulsators or F+1O double-mode pulsators, but never single mode fundamental pulsators. This property is the same in the case of Cepheids and in the case of RR Lyrae stars.

(v) In neither RR Lyrae stars nor Cepheids can the period ratio of ∼0.61 be reproduced by two radial modes. In both types of variables the secondary mode must be non-radial.

(vi) In every *Kepler* RRc star we detect at least one subharmonic of the secondary mode, at $\sim 1/2f_2$ or at $\sim 3/2f_2$. Similar subharmonics have also been found recently in several other RRc and RRd variables observed from space (Molnár et al., in preparation). They have also been retrospectively identified in two more RRd stars observed from space. Detection of subharmonics of f_2 is a signature of period doubling of this mode. After RV Tauri, Blazhko RRab and BL Herculis stars, the RRc and RRd stars are now the fourth group of pulsators in which period doubling has been found. Contrary to the former three types of variables, in the RRc and RRd stars the period doubling affects not the primary, but the secondary mode of pulsation.

(vii) Judging from the results of space photometric observations, the excitation of the secondary mode with the period ratio of ∼0.61 to the first overtone and concomitant period doubling of this mode must be a common phenomenon in RRc and RRd variables.

(viii) In every *Kepler* RRc star the amplitude and phase of the secondary mode and its subharmonics are strongly variable, with time-scales of 10–200 d. The main radial mode varies on the same time-scale, but with an extremely low amplitude. Its variability can be detected only with high-precision photometry collected from space.

(ix) In three *Kepler* RRc stars even more periodicities are detected, all with amplitudes well below 1 mmag. One of the low-amplitude modes discovered in KIC 5520878 can be identified with the radial second overtone, but all others must be non-radial. Many of these modes appear at frequencies that are below that of the radial fundamental mode. As such, they cannot be acoustic oscillations (p-modes), but must be classified as gravity modes (g-modes). This is the first detection of such modes in the RR Lyrae stars. The result is very surprising. From the theoretical point of view, the g-modes are not expected to be excited in the RR Lyrae variables, because they are all strongly damped in the radiative interior of the star.

At the time of writing, several additional RR Lyrae stars have been found in the *Kepler* field, thanks to the efforts of many dedicated individuals, and often as a by-product of studies devoted to other objects. For example, short period eclipsing binaries can have periods and amplitudes in the range of RR Lyrae stars (e.g. Rappaport et al. 2013; Szabó et al., in preparation) . Also, the citizen science project PlanetHunters (www.planethunters.org) has yielded some additional RR Lyrae stars in the *Kepler* field. Among the new finds are several RRc stars.

The sample of space-observed RRc and RRd variables will be further expanded by the *Kepler* K2 mission, which is already underway (Howell et al. 2014). It is observing in the plane of the ecliptic, and will switch the field of view every three months. With this strategy, a variety of stellar populations will be sampled, including not only the Galactic halo and the thick disc but also several globular clusters and the Galactic Bulge. The K2 mission can observe hundreds of RR Lyrae variables, among them tens of RRc and of RRd type (Molnár, Plachy & Szabó 2014). The mission will increase greatly the number such objects studied from space. It will be interesting to see whether they show characteristics similar to the four RRc variables discussed in this paper.

When writing of this manuscript was almost completed, a new paper on RRc stars has been submitted by Netzel, Smolec & Moskalik (2014). The authors have analysed the OGLE-III photometry of the Galactic Bulge. In ∼3 per cent of the studied variables, they have detected a low-amplitude secondary mode with the period ratio of ∼0.61 to the first radial overtone. This result confirms our conclusion that excitation of this puzzling mode is a common phenomenon in RRc stars.

ACKNOWLEDGEMENTS

Funding for this Discovery mission was provided by NASA's Science Mission Directorate. The authors gratefully acknowledge the entire *Kepler* team, whose outstanding efforts have made these results possible. This research has been supported by the Polish NCN through grant no. DEC-2012/05/B/ST9/03932. It has also been supported by the 'Lendület-2009 Young Researchers' Program of the Hungarian Academy of Sciences, the Hungarian OTKA grant K83790, the National Science Foundation grant no. NSF PHY05-51164, the European Community's Seventh Framework Programme (FP7/2007-2013) grants no. 269194 (IRSES/ASK), 312844 (SPACEINN) and 338251 (StellarAges), the ESA PECS Contract no. 4000110889/14/NL/NDe, the Ministry of Science and Technology (Taiwan) grant no. MOST101-2112-M-008-017-MY3, the Korea Astronomy and Space Science Institute Project no. 2014-1-400-06, supervised by the Ministry of Science, ICT and Future Planning and by the Polish NCN grant no. 2011/03/B/ST9/02667. KK is currently a Marie Curie Fellow, grateful for the support of grant PIOF-GA-2009-255267 (SAS-RRL). RSz acknowledges the University of Sydney IRCA grant. JMN wishes to thank the Camosun College Faculty Association for financial assistance.

REFERENCES

Bailey S. I., 1902, Harv. Coll. Observ. Ann., 38, 1
Benkő J. M. et al., 2010, MNRAS, 409, 1585
Benkő J. M., Szabó R., Paparó M., 2011, MNRAS, 417, 974
Benkő J. M., Plachy E., Szabó R., Molnár L., Kolláth Z., 2014, ApJS, 213, 31
Berdnikov L. N., Ignatova V. V., Pastukhova E. N., Turner D. G., 1997, Astron. Lett., 23, 177
Bergé P., Pomeau Y., Vidal Ch., 1986, Order within Chaos. Wiley, New York
Blazhko S., 1907, Astron. Nachr., 175, 325
Borucki W. J. et al., 2010, Science, 327, 977
Bowman D. M., Kurtz D. W., 2014, MNRAS, 444, 1909
Brown T. M., Latham D. W., Everett M. E., Esquerdo G. A., 2011, AJ, 142, 112
Buchler J. R., Kovács G., 1987, ApJ, 320, L57
Buchler J. R., Moskalik P., 1992, ApJ, 391, 736
Caldwell D. A. et al., 2010, ApJ, 713, L92
Chadid M., 2012, A&A, 540, A68
Derekas A., Kiss L. L., Udalski A., Bedding T. R., Szatmáry K., 2004, MNRAS, 354, 821
Dziembowski W. A., 2012, Acta Astron., 62, 323
Dziembowski W. A., Cassisi S., 1999, Acta Astron., 49, 371
Dziembowski W. A., Smolec R., 2009, in Guzik J. A., Pradley P. A., eds, AIP Conf. Proc. Vol. 1170, Stellar Pulsation: Challenges for Theory and Observation. Am. Inst. Phys., New York, p. 83
Gilliland R. L. et al., 2010, ApJ, 713, L160
Gruberbauer M. et al., 2007, MNRAS, 379, 1498

Guggenberger E. et al., 2012, MNRAS, 424, 649
Haas M. R. et al., 2010, ApJ, 713, L115
Howell S. B. et al., 2014, PASP, 126, 398
Jenkins J. M. et al., 2010a, ApJ, 713, L87
Jenkins J. M. et al., 2010b, ApJ, 713, L120
Jurcsik J., Clement C., Geyer E. H., Domsa I., 2001, AJ, 121, 951
Jurcsik J. et al., 2009, MNRAS, 400, 1006
Jurcsik J. et al., 2012, MNRAS, 419, 2173
Koch D. G. et al., 2010, ApJ, 713, L79
Kolenberg K. et al., 2010, ApJ, 713, L198
Kolenberg K. et al., 2011, MNRAS, 411, 878
Kolenberg K., Kurucz R. L., Stellingwerf R., Nemec J. M., Moskalik P., Fossati L., Barnes T. G., 2014, in Guzik J. A., Chaplin W. J., Handler G., Pigulski A., eds, Proc. IAU Symp. Vol. 301, Precision Asteroseismology. Cambridge Univ. Press, Cambridge, p. 257
Kolláth Z., Buchler J. R., Szabó R., Csurby Z., 2002, A&A, 385, 932
Kolláth Z., Molnár L., Szabó R., 2011, MNRAS, 414, 1111
Kovács G., 2001, in Takeuti M., Sasselov D. D., eds, Astrophys. Space Sci. Library, Vol. 257, Stellar Pulsation – Nonlinear Studies. Kluwer, Dordrecht, p. 61
Kovács G., Buchler J. R., 1988, ApJ, 334, 971
Kovács G., Buchler J. R., Davis C. G., 1987, ApJ, 319, 247
Le Borgne J. F. et al., 2007, A&A, 476, 307
Lub J., 1977, A&AS, 29, 345
Mizerski T., 2003, Acta Astron., 53, 307
Molnár L., Kolláth Z., Szabó R., Bryson S., Kolenberg K., Mullally F., Thompson S. E., 2012, ApJ, 757, L13
Molnár L., Plachy E., Szabó R., 2014, Inf. Bull. Var. Stars, 6108
Morgan S. M., Simet M., Bargenquast S., 1998, Acta Astron., 48, 341
Moskalik P., 2013, in Suárez J. C., Garrido R., Balona L. A., Christensen-Dalsgaard J., eds, Astrophysics and Space Science Proc. 31, Stellar Pulsations. Springer-Verlag, Berlin, p. 103
Moskalik P., 2014, in Guzik J. A., Chaplin W. J., Handler G., Pigulski A., eds, Proc. IAU Symp. Vol. 301, Precision Asteroseismology. Cambridge Univ. Press, Cambridge, p. 249
Moskalik P., Buchler J. R., 1990, ApJ, 355, 590
Moskalik P., Kołaczkowski Z., 2008, Commun. Asteroseismol., 157, 343
Moskalik P., Kołaczkowski Z., 2009, MNRAS, 394, 1649
Moskalik P. et al., 2013, in Suárez J. C., Garrido R., Balona L. A., Christensen-Dalsgaard J., eds, Astrophysics and Space Science Proc. 31, Stellar Pulsations. Springer-Verlag, Berlin, Poster 34 (arXiv:1208.4251)
Nagy A., Kovács G., 2006, A&A, 454, 257
Nemec J. M. et al., 2011, MNRAS, 417, 1022
Nemec J. M., Cohen J. G., Ripepi V., Derekas A., Moskalik P., Sesar B., Chadid M., Bruntt H., 2013, ApJ, 773, 181
Netzel H., Smolec R., Moskalik P., 2014, MNRAS, preprint (arXiv:1411.3155)
Olech A., Moskalik P., 2009, A&A, 494, L17
Olech A., Kaluzny J., Thompson I. B., Pych W., Krzemiński W., Schwarzenberg-Czerny A., 2001, MNRAS, 321, 421
Payne-Gaposchkin C., Gaposchkin S., 1966, Smithsonian Contrib. Astrophys., 9 1
Pigulski A., 2014, in Guzik J. A., Chaplin W. J., Handler G., Pigulski A., eds, Proc. IAU Symp. Vol. 301, Precision Asteroseismology. Cambridge Univ. Press, Cambridge, p. 31
Popielski B. L., Dziembowski W. A., Cassisi S., 2000, Acta Astron., 50, 491
Rappaport S., Deck K., Levine A., Borkovits T., Carter J., El Mellah I., Sanchis-Ojeda R., Kalomeni B., 2013, ApJ, 768, 33
Simon N., Lee A. S., 1981, ApJ, 248, 291
Smolec R., Moskalik P., 2008a, Acta Astron., 58, 193
Smolec R., Moskalik P., 2008b, Acta Astron., 58, 233
Smolec R., Moskalik P., 2010, A&A, 524, A40
Smolec R., Moskalik P., 2012, MNRAS, 426, 108
Smolec R. et al., 2012, MNRAS, 419, 2407
Soszyński I. et al., 2008, Acta Astron., 58, 163
Soszyński I. et al., 2009, Acta Astron., 59, 1
Soszyński I. et al., 2010, Acta Astron., 60, 17
Soszyński I. et al., 2011a, Acta Astron., 61, 1
Soszyński I. et al., 2011b, Acta Astron., 61, 285
Süveges M. et al., 2012, MNRAS, 424, 2528
Szabó R., 2014, in Guzik J. A., Chaplin W. J., Handler G., Pigulski A., eds, Proc. IAU Symp. 301, Precision Asteroseismology. Cambridge Univ. Press, Cambridge, p. 241
Szabó R. et al., 2010, MNRAS, 409, 1244
Szabó R. et al., 2014, A&A, 570, A100
Tsesevich V. P., 1975, in Kukarkin B. V., ed., Pulsating Stars. Wiley, New York, p. 144
Van Hoolst T., Dziembowski W. A., Kawaler S. D., 1998, MNRAS, 297, 536
Walker A. R., 1994, AJ, 108, 555

APPENDIX A: TIME-DEPENDENT PRE-WHITENING

In the standard pre-whitening procedure, a periodic signal is removed from the light curve by subtracting a sine function with constant frequency (f_1), amplitude (A_1) and phase (ϕ_1). The values of f_1, A_1 and ϕ_1 are determined from the data with a least-squares

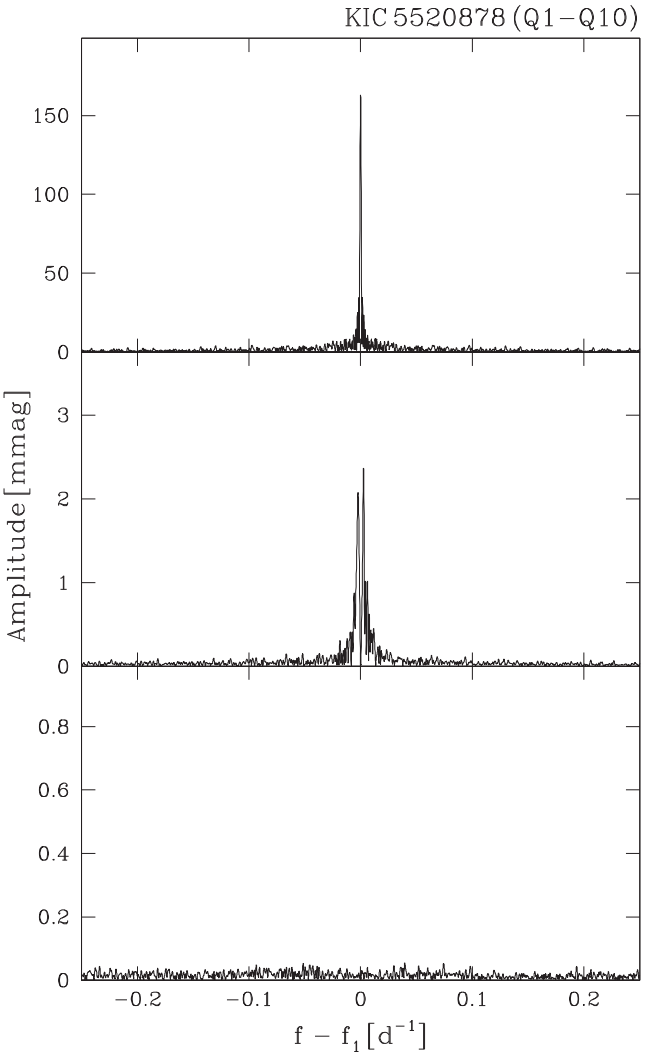

Figure A1. Pre-whitening of the main frequency in KIC 5520878. Upper panel: FT of the original *Kp* magnitude light curve (quarters Q1 – Q10). Middle panel: FT after standard pre-whitening. Bottom panel: FT after time-dependent pre-whitening ($\Delta t = 10$ d).

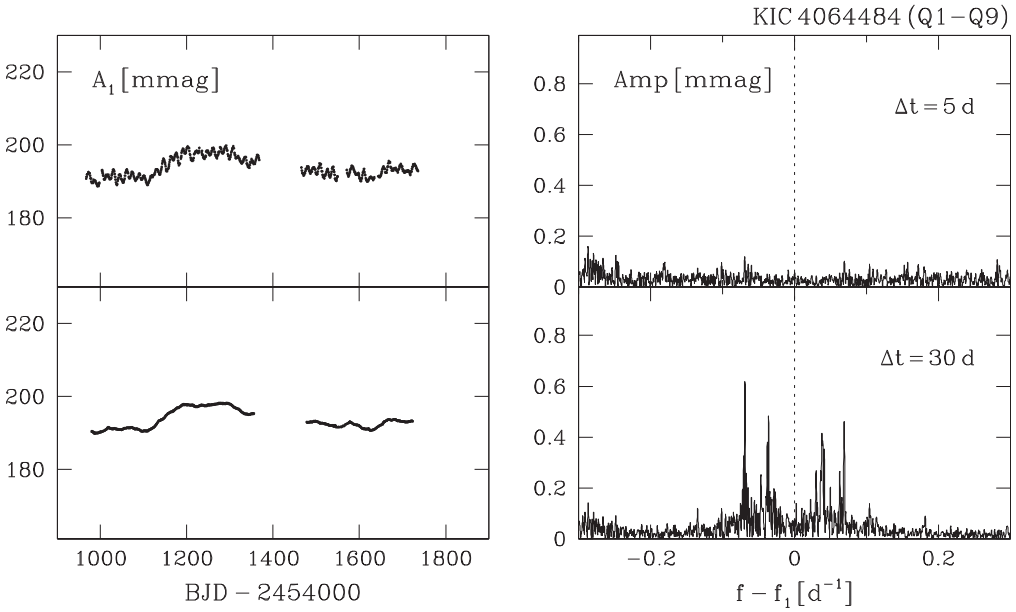

Figure A2. Time-dependent pre-whitening of the dominant mode of KIC 4064484 for the light-curve segment length of $\Delta t = 5$ d and 30 d. Left-hand column: variations of the amplitude of the mode, $A_1(t)$, determined with the time-dependent Fourier analysis. Right-hand column: FT of the pre-whitend light curve. Frequency of the removed dominant mode, f_1, is indicated by the dashed line.

fit. The method works very well when the signal's frequency, amplitude and phase are indeed non-variable. However, when this condition is violated, as is the case for the *Kepler* RRc stars, the standard procedure fails and leaves residual power in the frequency spectrum of the pre-whitened data. This is illustrated in Fig. A1, where we display the pre-whitening sequence for the dominant mode of KIC 5520878. The residuals in the FT (middle panel) have an amplitude of 2.4 mmag. This is only ∼1.5 per cent of the original peak's amplitude, but in context of *Kepler* photometry this is huge.

To remedy this situation, we have developed a novel method that we call the *time-dependent pre-whitening*. In this procedure, we subtract from the light curve a sine function not with constant, but with *varying* amplitude and phase. To model this variability, we adopt $A_1(t)$ and $\phi_1(t)$ determined from the data (Fig. 9) by the time-dependent Fourier analysis (Kovács et al. 1987). The frequency of the mode, f_1, is kept fixed. In the bottom panel of Fig. A1, we display the results of the time-dependent pre-whitening for KIC 5520878. The dominant frequency is now removed entirely, down to the noise level of the FT (55 μmag).

Time-dependent Fourier analysis and, consequently, also time-dependent pre-whitening, have one free parameter: the length of the light-curve segment, Δt. The choice of this parameter determines the time resolution of the method. Variations occurring on time-scales shorter than Δt will not be captured by the time-dependent Fourier analysis and consequently, they will not be subtracted by the pre-whitening procedure.

We illustrate this property in Fig. A2, where we present pre-whitening of the dominant frequency of KIC 4064484. In the upper panel we plot the results for $\Delta t = 5$ d. The time-dependent Fourier analysis (left-hand column) captures both the long-term trend and the rapid quasi-periodic modulation of the amplitude. Using this $A_1(t)$ and concomitant $\phi_1(t)$ (not shown), the time-dependent pre-whitening removes from the FT all power associated with the mode (right-hand column). The results for $\Delta t = 30$ d are quite different. The time-dependent Fourier analysis now captures only the long-term trend, but the rapid modulation is averaged out. After the time-dependent pre-whitening, we find four residual peaks in the FT. They are placed symmetrically around the (removed) central frequency, f_1, forming an equidistant frequency multiplet. These peaks are the Fourier representation of the quasi-periodic modulation of the mode, which for $\Delta t = 30$ d is not captured by the method and not removed during pre-whitening.

In the language of the Fourier analysis, $\Delta t = 5$ d corresponds to a bandwidth of 0.2 d^{-1} ($1/\Delta t$). This is broader than the frequency multiplet in Fig. A2. As a result, the signal reconstructed with the time-dependent Fourier analysis captures *all* the Fourier power associated with the mode and *all* of it can be removed. For $\Delta t = 30$ d, the bandwidth is only 0.0333 d^{-1}. This is narrow enough to isolate only the central peak of the multiplet. Consequently, only this peak is subtracted in the pre-whitening process.

This paper has been typeset from a TEX/LATEX file prepared by the author.